

CERN-EP-2026-046  
23 February 2026

## $\pi$ , K, and p production in high-multiplicity pp collisions at $\sqrt{s} = 13$ TeV

ALICE Collaboration\*

### Abstract

This paper presents the measurement of  $\pi^\pm$ ,  $K^\pm$ , and  $p(\bar{p})$  production in high-multiplicity proton–proton collisions at  $\sqrt{s} = 13$  TeV at midrapidity ( $|y| < 0.5$ ) using the ALICE detector at the LHC. The transverse-momentum ( $p_T$ ) spectra of these particles are reported for three high-multiplicity classes. The results show a mass- and multiplicity-dependent hardening of the  $p_T$  spectra and an enhancement of the  $p/\pi$  ratio at intermediate  $p_T$ . These features are similar to those observed in heavy-ion collisions, where quark–gluon plasma formation is expected. The new measurements have extended the highest average charged-particle multiplicity density per unit of pseudorapidity achieved in pp collisions, roughly a factor five higher than that in average inelastic pp collisions, thereby reducing the multiplicity gap between small and large collision systems. In addition, the results are further compared with previously published measurements and with model calculations obtained using distinct tunes of the PYTHIA 8 Monte Carlo generator, as well as with predictions from the EPOS4. The comparison of the  $p_T$ -integrated  $K/\pi$  and  $p/\pi$  ratios across different collision systems and energies suggests that particle production scales with charged-particle multiplicity, rather than with collision energy or system size. While the PYTHIA 8 tunes and the EPOS4 model are able to reproduce some of these measurements, either quantitatively or qualitatively, none of them consistently describes all observed features of the data.

arXiv:2603.13203v1 [nucl-ex] 13 Mar 2026

© 2026 CERN for the benefit of the ALICE Collaboration.

Reproduction of this article or parts of it is allowed as specified in the CC-BY-4.0 license.

---

\*See Appendix A for the list of collaboration members

## 1 Introduction

In high-energy nucleus–nucleus (AA) collisions, a hot and dense state of deconfined, strongly interacting matter, known as quark–gluon plasma (QGP), is formed [1]. The ultrarelativistic energies available at the Large Hadron Collider (LHC) provide a unique opportunity to explore its properties. This system undergoes a hydrodynamic evolution [2–4] and exhibits an enhanced production of (multi-)strange hadrons, long-range angular correlations, non-zero anisotropic flow harmonics, and suppression of high transverse momentum ( $p_T$ ) particles in the dense medium as measured by the nuclear-modification factor [5–7]. The light-flavor hadrons produced at low  $p_T$ , created through soft parton interactions, provide essential insights into the collective behavior in the QGP [8].

The observation of a “ridge-like” structure in angular correlations between produced particles, as well as non-zero anisotropic flow coefficients, has also been reported in small systems such as proton–proton (pp) and proton–lead (p–Pb) collisions [9–12]. Studies of high-multiplicity (HM) pp and p–Pb collisions have revealed several key features that resemble those observed in heavier collision systems, where the formation of the QGP is well established. These features include the observation of mass-dependent hardening of  $p_T$  spectra, the increase of average transverse momentum ( $\langle p_T \rangle$ ) with multiplicity, strangeness enhancement, and an enhanced baryon-to-meson ratio at intermediate  $p_T$  [13–20]. Despite these similarities, the nuclear modification factor remains consistent with unity at high  $p_T$ . This contrasts with the suppression observed in heavy-ion collisions. The nuclear modification factor represents the ratio of particle yields measured in lead–lead (Pb–Pb) or p–Pb collisions to those in pp collisions scaled by the number of binary nucleon–nucleon collisions [21, 22].

The study of hadron-to-pion ratios as a function of the average charged-particle multiplicity ( $\langle dN_{\text{ch}}/d\eta \rangle$ ) from pp to p–Pb and then to Pb–Pb system suggested that the particle production depends primarily on charged-particle multiplicity, independent of collision system or energy [13, 20]. This observation raises the question of whether there are common physical mechanisms in small and large systems.

To investigate the origin of collective-like effects in pp collisions, it is essential to use observables that are sensitive to these phenomena and to compare the results with theoretical model predictions. In particular, the transverse momentum spectra of identified particles provide important information, e.g., the mass-dependent spectral shape and mass ordering, which are commonly associated with radial flow [20]. Since collective phenomena in pp and p–Pb collisions can not be derived directly from first-principle Quantum Chromodynamics (QCD), their description often relies on phenomenological models [23–27]. PYTHIA, a Monte Carlo (MC) event generator based on the Lund string model [28], is able to generate high-multiplicity pp events with color reconnection, enhanced strangeness production [13], radial-like expansion via color-rope fragmentation [29, 30], and anisotropies in the final-state momentum distributions arising from repulsive interactions among color strings (string shoving) [31]. In addition, color-reconnection schemes beyond the leading-color (CLR-BLC) approximation introduce string junction topologies and provide a good description of the  $p/\pi$  ratio at low  $p_T$  in minimum bias (MB) pp collisions [32]. The EPOS4 model implements a core-corona approach [33, 34], in which strings in low-density regions fragment to form the corona, while the high-density core undergoes collective expansion. This approach is able to describe certain collective-like features, such as radial flow and strangeness enhancement, in small collision systems [35]. However, none of these theoretical approaches provides a consistent quantitative description of the collective-like effects in small collision systems [10, 20, 36]. Small collision systems at the highest charged-particle multiplicities therefore offer essential input for constraining and improving existing theoretical models.

In this article, we present the measurements of primary charged particles, i.e.  $\pi^\pm$ ,  $K^\pm$ , and  $p(\bar{p})$  at midrapidity ( $|y| < 0.5$ ) in pp collisions at  $\sqrt{s} = 13$  TeV across three high-multiplicity classes using the ALICE detector [37, 38]. PYTHIA 8 and EPOS4 are used as reference models for comparison with the experimental results. The new results extend the previous measurements of light-flavor hadron production

from an average charged-particle multiplicity of 26.0 to 35.8, thus reducing the gap between pp and large collision systems. At such high multiplicities, pp events reach charged-particle densities that are comparable to those observed in peripheral (70–80%) Pb–Pb collisions at  $\sqrt{s_{NN}} = 2.76$  TeV [39]. This paper is organized as follows: Section 2 describes the ALICE experimental setup and data analysis. The results, along with model predictions, are presented and discussed in Section 3. Finally, the paper is summarized in Section 4.

## 2 Experimental setup and data analysis

### 2.1 The ALICE detector

A detailed description of the ALICE apparatus, as well as its performance, can be found in Refs. [37, 40]. The detector configuration used in this analysis corresponds to the Run 2 setup prior to the Long Shutdown 2 upgrade. The main detectors used in this analysis are the V0 [37], the Inner Tracking System (ITS) [41], the Time Projection Chamber (TPC) [42], and the Time-Of-Flight (TOF) [43]. All of these detectors are located inside a 0.5 T solenoid magnetic field.

The V0 detector is used for triggering, multiplicity estimation, and background suppression. It consists of two scintillator arrays positioned along the beam axis on either side of the interaction point (IP), located at  $z = 340$  cm (V0A) and  $z = -90$  cm (V0C). These arrays cover the pseudorapidity ranges  $2.8 < \eta < 5.1$  and  $-3.7 < \eta < -1.7$  for V0A and V0C, respectively. The V0M multiplicity estimator obtained from the combination of V0A and V0C signals is used to classify events according to their measured multiplicity [19].

The ITS is the tracking device closest to the interaction point. It is composed of six cylindrical layers of high-resolution silicon detectors, covering a pseudorapidity range of  $|\eta| < 0.9$ . The two innermost layers of ITS consist of hybrid Silicon Pixel Detectors (SPD), located at a radial distance of 3.9 cm and 7.6 cm from the beam axis, covering pseudorapidity ranges of  $|\eta| < 2$  and  $|\eta| < 1.4$ , respectively. The outer four layers are composed of Silicon Strip (SSD) and Silicon Drift (SDD) Detectors, which are also used to identify particles by measuring the specific energy loss ( $dE/dx$ ) at low transverse momentum.

The TPC, together with the ITS [42], is the main tracking detector of the ALICE central barrel and covers the same pseudorapidity range as the ITS. It is a gaseous detector with radial and longitudinal dimensions of approximately  $85 \text{ cm} < r < 247 \text{ cm}$  and  $|z| < 250 \text{ cm}$ , respectively. The TPC identifies charged particles through the measurement of their specific energy loss and provides three-dimensional spatial information for each track, with up to 159 samples per track.

The TOF [43] detector is based on the Multigap Resistive Plate Chamber (MRPC) technology. It covers the full azimuthal range for the pseudorapidity interval  $|\eta| < 0.9$  and is cylindrically symmetric at an average distance of  $\sim 4$  m from the beam axis. The TOF detector identifies charged particles by measuring their time of flight. Since particles and antiparticles are produced in equal amounts at LHC energies [44], for the rest of this paper, we will use the notation  $\pi$ , K, and p to denote  $(\pi^+ + \pi^-)$ ,  $(K^+ + K^-)$ , and  $(p + \bar{p})$ , respectively.

### 2.2 Data sample, event and track selection

The results presented in this paper are obtained by combining two independent analyses, namely ITS stand-alone (ITSsa) and TPC–TOF. The analyzed data correspond to pp collisions at  $\sqrt{s} = 13$  TeV collected during the LHC Run 2 in 2016, with an integrated luminosity of  $13 \text{ pb}^{-1}$  for the HM-triggered sample. After all event selections, approximately  $8 \times 10^7$  and  $8 \times 10^6$  events are used for the ITSsa and TPC–TOF analyses, respectively. High-multiplicity events are selected using the HM trigger, which is defined by a threshold on the relative V0M amplitude with respect to its average value  $V0M/\langle V0M \rangle \gtrsim 4.9$ , selecting the top 0.1% of the minimum bias events [45, 46]. Additionally, accepted events are required

to have a primary vertex in the fiducial region  $|z| < 10$  cm. The events with out-of-bunch pileup were removed using timing information from the V0 counter. In-bunch pileup was identified using the SPD and removed from the analysis [40]. The fraction of rejected events does not exceed about 3%, and its impact on the measured spectra is negligible [47].

For the measurement of  $\pi$ , K, and p spectra, we divided the high-multiplicity data into three classes: HM I, HM II, and HM III, corresponding to the top 0–0.01%, 0.01–0.05%, and 0.05–0.1% of the  $V0M/\langle V0M \rangle$  signal percentile, respectively. The corresponding average charged-particle multiplicity densities ( $\langle dN_{ch}/d\eta \rangle$ ), defined as the total number of charged particles produced per unit pseudorapidity in the  $|\eta| < 0.5$  window [48], are listed in Tab. 1.

**Table 1:** Average charged-particle multiplicity density  $\langle dN_{ch}/d\eta \rangle$  measured in the three event multiplicity classes used in this analysis.

Multiplicity class	$\sigma/\sigma_{\text{INEL}>0}$ (%)	$\langle dN_{ch}/d\eta \rangle_{ \eta <0.5}$
HM I	0 – 0.01	$35.8 \pm 0.5$
HM II	0.01 – 0.05	$32.2 \pm 0.4$
HM III	0.05 – 0.1	$30.1 \pm 0.4$

The tracks were selected using track-selection criteria similar to those described in Ref. [19]. Analyzed tracks are restricted to the pseudorapidity region  $|\eta| < 0.8$  to ensure good acceptance and performance. To ensure good track selection, we require at least 70 traversed TPC readout rows; the tracks are selected having goodness-of-fit,  $\chi^2$  per TPC cluster (hits), to be less than 4. The track’s distance of closest approach (DCA) to the primary vertex along the longitudinal axis must satisfy  $DCA_z < 2$  cm, and in the transverse plane ( $DCA_{xy}$ ), it is required to satisfy a  $p_T$ -dependent cut of less than 7 times the DCA resolution. ITSsa tracks are required to have at least four ITS clusters, including at least one in the SPD layers, and at least three in the SDD or SSD layers, with  $\chi^2$  per ITS cluster required to be less than 2.5.

### 2.3 Particle identification

Particle identification (PID) is performed using the specific energy loss ( $dE/dx$ ) measured by the ITS and TPC, and the time-of-flight measured in the TOF. Low- $p_T$  particles (typically 0.1–0.75 GeV/ $c$  depending on the particle species) are reconstructed using a dedicated tracking algorithm which only uses the ITS information. In the ITSsa, hadron identification is performed by calculating the energy loss measured in three or four outer ITS layers [40]. The difference between the measured and expected value of  $dE/dx$  for each type of particle is calculated in multiples of standard deviations  $\sigma$ . The detailed description of this method is provided in Ref. [19].

In the relatively higher  $p_T$  region (0.6–4.0 GeV/ $c$ , or 0.7–4.0 GeV/ $c$  depending on particle species), particle identification is performed using a TPC–TOF two-dimensional (2D) fit method. This method is illustrated in Fig. 1. For each particle species  $i$  (pions, kaons, and protons), the  $y$  axis shows  $X_i = dE/dx - \langle dE/dx \rangle_i$  obtained from the TPC [19] and the  $x$  axis represents  $T_i = \Delta t - \langle \Delta t \rangle_i$  provided by the TOF [49]. Here,  $dE/dx$  and  $\Delta t$  are the measured specific energy loss in the TPC detector and time of flight in the TOF detector, respectively. The terms  $\langle dE/dx \rangle_i$  and  $\langle \Delta t \rangle_i$  correspond to their expected values for a given  $p_T$  range.

To extract the raw yield for each particle species in various  $p_T$  intervals, a fit is performed on the  $(T_i, X_i)$  distribution using the following fit functions.

$$\frac{d^2 N_{\text{tot}}}{dT_i dX_i} = \sum_j \frac{d^2 N_j}{dT_i dX_i} + M_i, \quad (1)$$

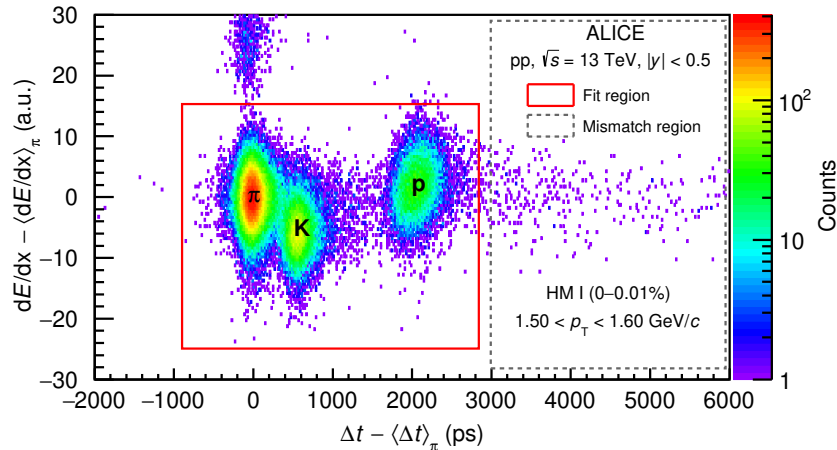


**Figure 1:** Difference between measured  $dE/dx$  (in the TPC) and its expected value for pions as a function of the same difference in time of flight as obtained from TOF. The plot is shown for  $1.50 < p_T < 1.60$  GeV/c at midrapidity. The red box represents the regions of the 2D fit, while the gray dashed box indicates the mismatch region.

where

$$\frac{d^2N_j}{dT_i dX_i} \propto \frac{dN_j}{dT_i} \times \frac{dN_j}{dX_i} \quad (2)$$

and  $M_i$  stands for the mismatch component that accounts for the background from wrongly associated TOF signals (TOF mismatches). Here,  $i$  corresponds to the particle species under study, and  $j$  runs over all the species (pions, kaons, and protons). The TOF mismatch is modeled using a data-driven template histogram constructed by randomly assigning TOF signals to reconstructed tracks [39]. Figure 1 shows an example of  $(T_i, X_i)$  distribution for  $1.50 < p_T < 1.60$  GeV/c under the pion mass assumption for the HM I multiplicity class. The various regions represent the different particle species, with pions located at  $(0,0)$ . The regions corresponding to other particles are separated due to the difference between their masses and the assumed pion-mass hypothesis. The red box represents the region of simultaneous fit for the TPC and TOF responses, while the gray dashed box indicates the mismatch region. The best fitting parameters are obtained by maximizing the logarithm of the likelihood of the fit function, and the raw yield for species  $i$  is extracted as the fit parameter.

## 2.4 Corrections and Normalization

The raw particle yields obtained from the ITSsa and TPC–TOF PID methods require various corrections, including tracking acceptance  $\times$  efficiency, TPC–TOF matching efficiency, and contamination from secondary particles. The resulting spectra are then normalized by the number of events in each multiplicity class to obtain the final  $p_T$ -spectra [19, 20, 50]. Tracking acceptance  $\times$  efficiency accounts for the particles lost due to the geometrical acceptance of the detector as well as its limited detection efficiency. The TPC–TOF matching efficiency takes into account that not all analyzed tracks have a hit in the TOF. It is calculated as the ratio of the total number of tracks matched with the TOF to the total number of tracks reconstructed by the TPC. These corrections are derived from simulated pp collision events, which are generated using the PYTHIA 8 model (Monash 2013 tune [24, 28]), and the interactions of the generated particles with the experimental apparatus are modeled using GEANT4 [51]. In the simulation, one applies the same track selection criteria used for the data to account for detector acceptance and reconstruction efficiencies. It is also observed that these efficiencies show negligible variation with charged-particle multiplicity, so the multiplicity-integrated values are used for these corrections.

In this article, we present the measurements of primary particles, referred to as prompt particles in colli-

sions, including decay products, except those from weak decays of strange particles and material interactions [52]. The contamination from secondary particles produced in the detector material mainly affects protons, while that from weak decays affects both pions and protons. In order to estimate the contribution from secondary particles, produced from the weak decays or material interactions, a template fit method is used. This method is based on the fact that the  $DCA_{xy}$  of primary particles, secondary particles from weak decays, and the secondaries from the material interactions are qualitatively different. Using the MC production, we obtain the corresponding  $DCA_{xy}$  template distributions. To obtain the correct fraction of the primary particles, we fitted the data with the fit templates as carried out in the previous work [20]. The contribution of the secondary particles for pions and protons is maximum at low  $p_T$  ( $\sim 2.5\%$  at 0.1 GeV/c for pions and 8.3% at 0.3 GeV/c for protons) and becomes negligible at higher  $p_T$ , while the contribution from kaons is negligible.

### 2.5 Systematic Uncertainties

The systematic uncertainties in this analysis arise from various sources across the  $p_T$  range. They are calculated by varying the selection criteria around the default values and comparing the resulting measurements with those obtained using the default criteria. A summary of these uncertainties is presented in Tab. 2. The final systematic uncertainty is obtained as the sum in quadrature of the uncertainties due

**Table 2:** Sources of systematic uncertainties on the corrected spectra. The uncertainties are split into two categories, the common and the individual-analysis specific. The symbol “–” (negl.) indicates that the source is not applicable (negligible) for the corresponding analysis.

$p_T$ (GeV/c)	Uncertainty (%)								
	$\pi$			K			p		
	0.1	0.75	4.0	0.2	0.6	4.0	0.3	0.7	4.0
	Common Source								
Correction for secondaries	1.0	1.0	1.0	negl.	negl.	negl.	4.0	4.0	4.0
Hadronic interactions	2.0	2.0	2.4	2.7	2.7	1.8	3.6	3.6	3.6
	ITSsa								
PID	0.4	0.4	–	3.3	3.3	–	3.6	3.6	–
Material budget	4.8	0.3	–	2.3	0.6	–	5.0	0.9	–
$E \times B$ effect	3.0	3.0	–	3.0	3.0	–	3.0	3.0	–
Tracking efficiency (ITSsa tracks)	2.8	2.8	–	2.9	2.9	–	5.2	5.2	–
	TPC–TOF								
ITS-TPC matching efficiency	–	0.7	1.5	–	–	1.5	–	–	1.5
PID	–	2.0	2.0	–	–	2.0	–	–	2.0
TOF-matching efficiency	–	3.0	3.0	–	–	6.0	–	–	4.0
Material budget	–	0.5	1.0	–	–	1.0	–	–	2.9
Global tracking efficiency (incl. track cut variation)	–	0.3	0.5	–	–	2.6	–	–	3.0
Total	7.1	6.7	5.3	6.7	6.4	7.6	10.4	9.3	8.5

to each variation. The sources of systematic uncertainties are divided into two parts: the first being common to ITSsa and TPC–TOF analyses, and the second specific to each analysis. The common sources of systematic uncertainty for both ITSsa and TPC–TOF analyses are the hadronic interaction cross section in the detector material and the corrections for secondary particles. The uncertainty associated with the hadronic interaction cross section in the detector material is evaluated using the GEANT4 [51] and

FLUKA [53] transport codes. Additionally, a 2% systematic uncertainty is included to account for possible multiplicity dependence effects in track reconstruction efficiency and signal loss correction derived from MC simulations [20]. The contamination from out-of-bunch pileup tracks in the ITS–TPC matching is negligible, and the high-interaction rate related uncertainties are negligible relative to the other systematics.

The ITSsa analysis includes the uncertainties arising from particle identification (PID), the ITS material budget, and the Lorentz force ( $E \times B$ ) effect. PID uncertainties are evaluated using a Bayesian approach and comparing the results obtained with the standard  $n\sigma$  method [21]. Material budget uncertainties are estimated by varying the ITS material by  $\pm 7.5\%$  [54]. The Lorentz force induces shifts in ITS cluster positions depending on the magnetic field polarity, resulting in an uncertainty of about 3%. All of these uncertainties are taken from Ref. [20]. A detailed description of the estimation of systematic uncertainties for the ITSsa analysis can be found in Refs. [19, 20]. The track selection uncertainties of ITSsa are obtained by varying the track selection criteria, mainly the  $DCA_{xy}$  and  $DCA_z$ , the  $\chi^2$  of the track and the number of ITS clusters.

The systematic uncertainties associated with TPC–TOF analysis include the uncertainties due to the ITS–TPC matching efficiency, PID, TOF-matching efficiency, material-budget, and tracking efficiency. The systematic uncertainties related to the ITS–TPC and TPC–TOF track matching are estimated by comparing the matching efficiencies in data and MC simulations. The material budget uncertainty is obtained by varying the material budget in the simulation by  $\pm 5\%$  [20]. The uncertainties associated with tracking are assessed by varying the track selection criteria, which mainly include the number of clusters in the TPC,  $DCA_{xy}$  and  $DCA_z$ . The uncertainties related to the particle identification are calculated by repeating the fits with varied fit ranges and parameters. The uncertainties listed in Tab. 2 are assumed to be uncorrelated among different particle species, except those arising due to the magnetic field polarity, ITS–TPC matching efficiency, and the multiplicity-dependent tracking efficiency and signal loss corrections. The systematic uncertainties on the  $p_T$ -integrated observables will be described in Sec. 3.3 in detail.

### 3 Results and discussion

#### 3.1 $p_T$ -differential results

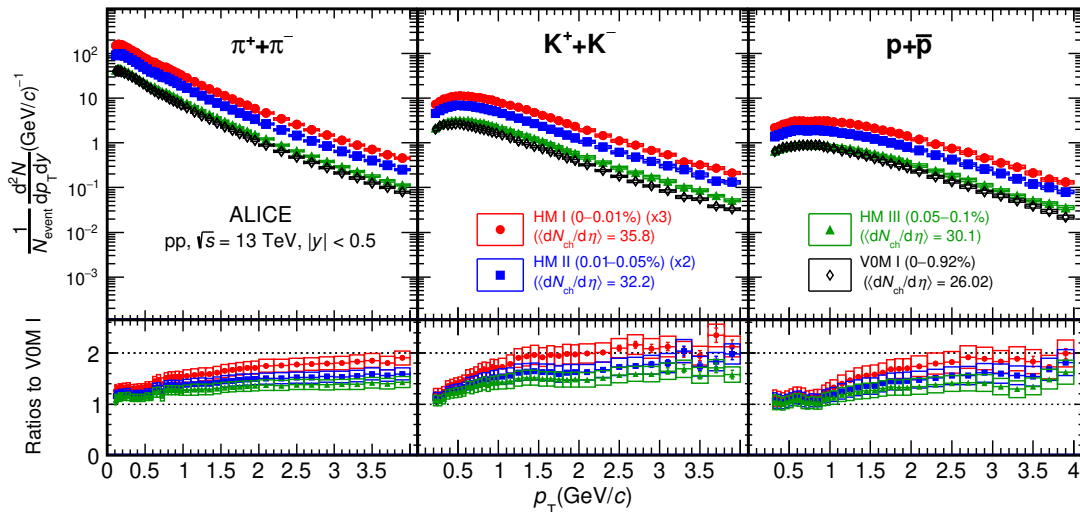


**Figure 2:** (Top panels) Transverse momentum spectra of  $\pi$ , K, and p for different multiplicity classes. Spectra are scaled to improve visibility. The corresponding ratios to V0M I (0–0.92%) spectrum [20] are shown in the bottom panels. Vertical bars and open boxes represent the statistical and systematic uncertainties, respectively.

The  $p_T$ -differential spectra of the species under study ( $\pi$ , K, and p) for the multiplicity classes reported in

Tab. 1 are shown in Fig. 2. In the overlapping  $p_T$  intervals, the ITSsa and TPC–TOF spectra are combined using a weighted average based on the inverse squared uncorrelated systematic uncertainties [49]. The bottom panels of Fig. 2 show the ratios of the spectra to the VOM I (0–0.92%) multiplicity class measured by ALICE [20]. For all the identified hadrons, the ratios show a hardening of the spectra with increasing multiplicity. Such observations have been previously reported in pp, p–Pb, and Pb–Pb collisions and are attributed to hydrodynamical evolution of the system [8, 18, 20].

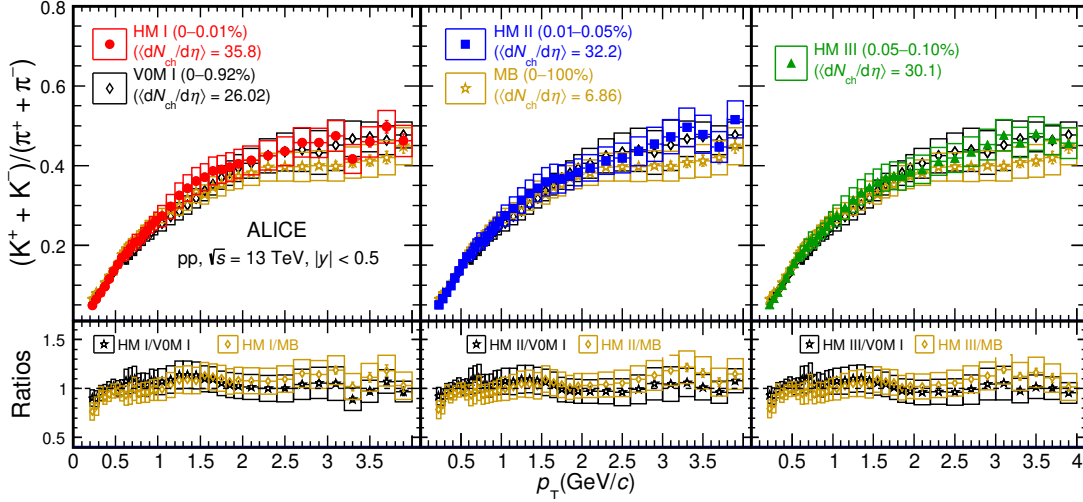


**Figure 3:** (Top panels)  $K/\pi$  spectrum ratios as a function of  $p_T$  for all three high-multiplicity classes, VOM I (0–0.92%) [20] and MB (0–100%) [50] multiplicity classes. The bottom panels show the ratio to the VOM I and MB classes. The boxes represent the systematic uncertainties, while the bars represent the statistical ones.

The relative production of different charged hadrons at various transverse momenta can be studied through the ratio of their  $p_T$ -differential spectra as a function of event multiplicity. The measured  $K/\pi$  ratio as a function of  $p_T$  for different multiplicity classes is shown in Fig. 3. The results are compared with

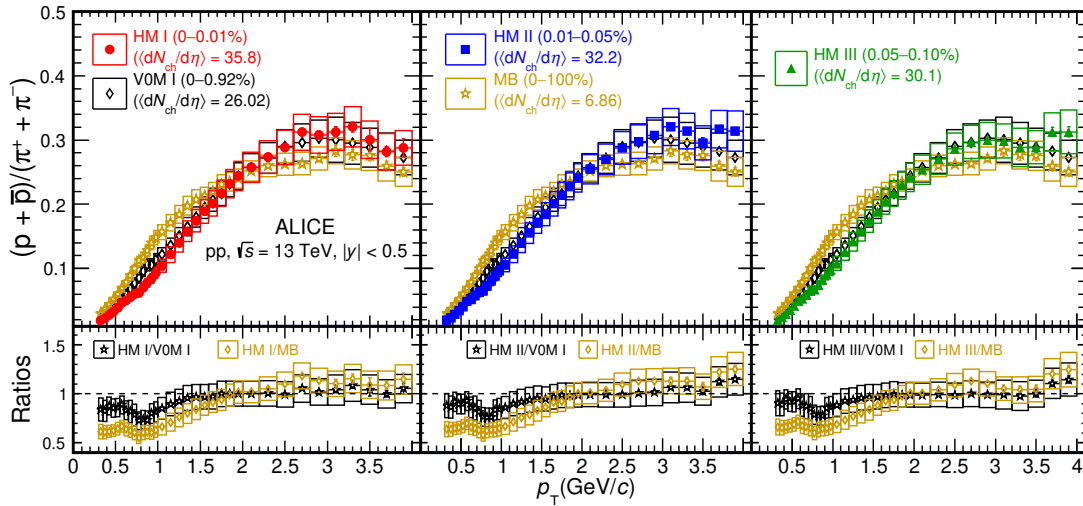


**Figure 4:** (Top panels)  $p/\pi$  spectrum ratios as a function of  $p_T$  for three high-multiplicity classes and VOM I (0–0.92%) [20] and minimum bias (MB) (0–100%) [50] multiplicity classes. The bottom panels show the ratio to the VOM I and MB classes. The boxes represent the systematic uncertainties, while the bars represent the statistical ones.

those from the VOM I [20] and MB [50] multiplicity classes measured in pp collisions at  $\sqrt{s} = 13$  TeV,

as shown in Fig. 3. The  $K/\pi$  ratio exhibits an increasing trend at low  $p_T$  and tends to saturate at higher  $p_T$ . The bottom panel shows the ratios of the measurements to V0M I and MB. The measurements are consistent with those of the V0M I and MB classes. Our measurements are also consistent with the previously published  $K/\pi$  ratio in peripheral (70–80%) Pb–Pb collisions at  $\sqrt{s_{NN}} = 2.76$  TeV and 5.02 TeV [8], which shows a steep increase with  $p_T$  from  $\sim 0.07$  at the lowest  $p_T$  and saturates at  $\sim 0.47$  toward higher  $p_T$ . Figure 4 shows the  $p/\pi$  ratio as a function of  $p_T$  for different multiplicity classes. The results are also compared with the V0M I and MB multiplicity classes. The bottom panels show the ratio of the results to the published ones. A suppression in the  $p/\pi$  ratio at low  $p_T$  ( $< 1$  GeV/c) and an enhancement at intermediate  $p_T$  ( $\sim 3$  GeV/c) is observed. The results show a systematically increasing trend from HM I to HM III, although the significance of this rise is low due to large uncertainties. A similar enhancement of  $p/\pi$  ratios at intermediate  $p_T$  has been observed in p–Pb and Pb–Pb collisions, where it has been associated with collective flow or quark recombination [8, 18, 39]. In addition, both the  $K/\pi$  and  $p/\pi$  ratios as a function of  $p_T$  show a hardening of the spectra which is more pronounced for the heavier particles, see Fig. 2. Quantitatively, the  $K/\pi$  ( $p/\pi$ ) ratio increases by a factor of about 6 (15) from  $p_T \sim 0.3$  to 3.0 GeV/c for the studied HM classes, suggesting a large increase for heavier particles (p).

### 3.2 Comparison of $p_T$ -differential results with models

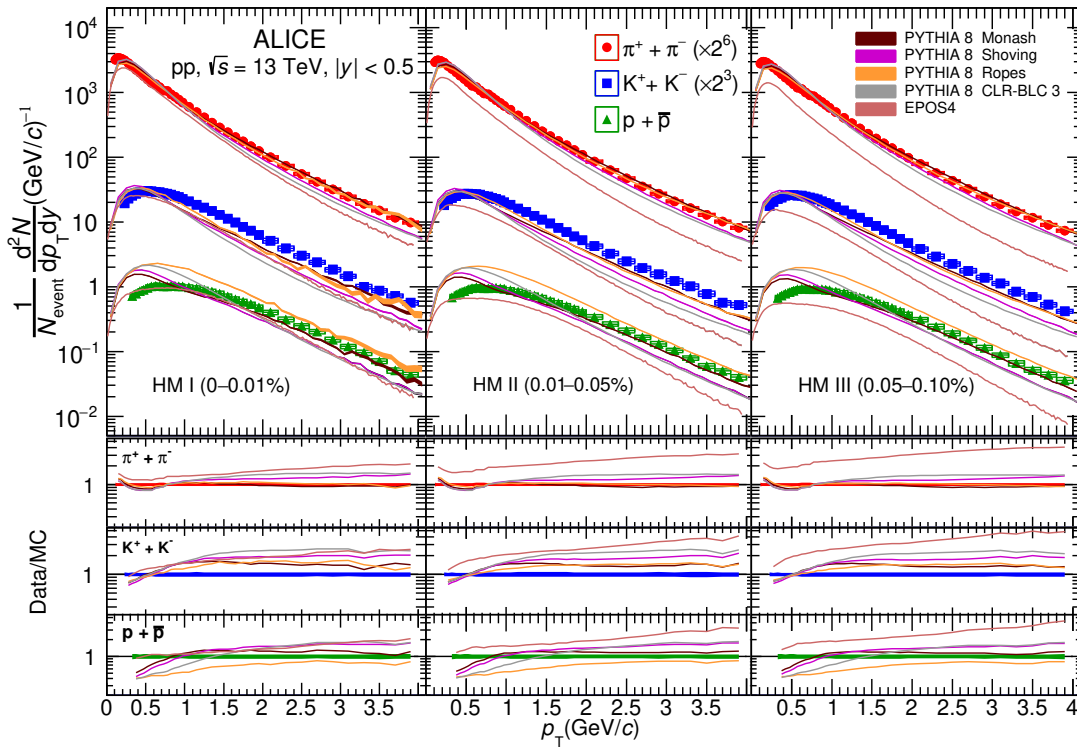


**Figure 5:** (Top panels) Measured  $p_T$  spectra of  $\pi$ , K, and p compared with PYTHIA 8 Monash, PYTHIA 8 Shoving, PYTHIA 8 Ropes, PYTHIA 8 CLR-BLC 3, and EPOS4 MC predictions for HM I (left), HM II (middle), and HM III (right) multiplicity classes. Statistical (bars) and systematic (open boxes) uncertainties are shown for the data. The shaded bands around the MC curves represent the statistical uncertainties of the model predictions. (Bottom panels) Ratio of the data to MC predictions. The bands around one in the bottom panels represent the systematic uncertainties of the data. Model uncertainties are not included in the ratio plots for better visibility.

The comparison between the measured  $p_T$  spectra of  $\pi$ , K, and p with pQCD-inspired MC event generator calculations provides valuable insight into the hadronization mechanism. Figure 5 presents a

comparison of the measured  $\pi$ , K, and p spectra with predictions from different tunes of the PYTHIA 8 model, namely the Monash 2013 tune [24], Ropes [55], Shoving [31], and CLR-BLC 3 [56], as well as with predictions from the EPOS4 model [33], for different multiplicity classes.

PYTHIA 8 is based on the Lund String Model [57, 58], which describes hadronization through the fragmentation of QCD strings into hadrons. PYTHIA 8 with the Monash 2013 tune implements MPI and a basic version of the Color-Reconnection mechanism. PYTHIA 8 with ropes results in a higher effective string tension due to the overlap of several strings at the hadronization time (color ropes), leading to an increased production of baryons and strangeness [55]. PYTHIA 8 with shoving tune accounts for string interactions, where strings repel each other in the transverse direction. This interaction generates microscopic transverse pressure, leading to long-range correlations [59]. In PYTHIA 8, the CLR-BLC approximation implements the formation of string junction topologies during the color-reconnection stage, which subsequently leads to enhanced baryon production during string fragmentation. The PYTHIA 8 CLR-BLC model provides several modes (0, 2, and 3) that impose different time-dilation and causality constraints on string reconnection before hadronization [56]. As discussed in recent studies, the Mode 3 provides a good description of the  $p/\pi$  ratio at low  $p_T$  in MB pp collisions [32]. Accordingly, the CLR-BLC Mode 3 tune is compared with data and other models in high-multiplicity pp events. EPOS4, the latest version of the EPOS event generator, implements initial partonic scatterings using a Pomeron-based Gribov–Regge scheme and dynamically separates the system into a dense ‘core’ and a dilute ‘corona’ [33, 34]. In these predictions, event classes are determined based on the number of charged particles simulated at both forward and backward pseudorapidities within the V0 detector coverage, using a method similar to that employed for data classification. Then, the  $\langle dN_{ch}/d\eta \rangle$  is determined in the central pseudorapidity region  $|\eta| < 0.5$ .

It is observed from Fig. 5 that the measured  $p_T$  spectra of pions are qualitatively reproduced by the PYTHIA 8 Monash and PYTHIA 8 Ropes tunings within about 20% over the full  $p_T$  range, while the EPOS4 underestimates the spectra over the entire range. The comparisons of the  $K/\pi$  and  $p/\pi$  ratios, with PYTHIA 8 and EPOS4 model predictions are shown in Fig. 6. All MC calculations underestimate

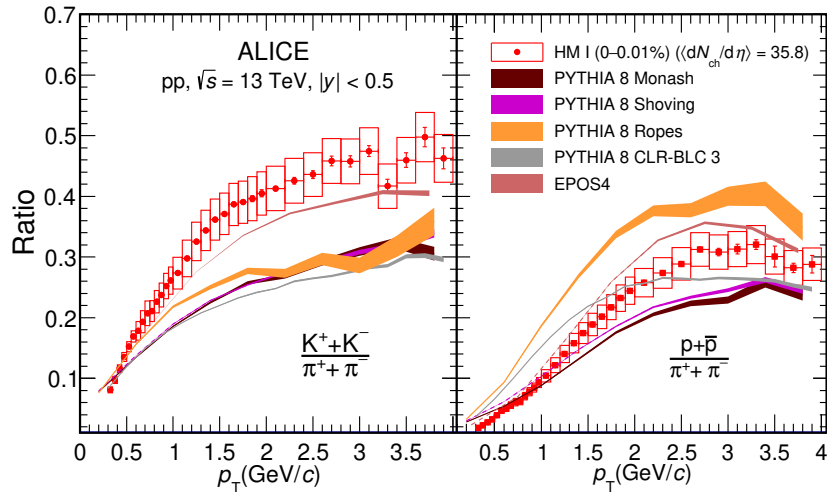


**Figure 6:**  $(K^+ + K^-)/(\pi^+ + \pi^-)$  (left) and  $(p + \bar{p})/(\pi^+ + \pi^-)$  (right) ratios in pp collisions as a function of  $p_T$  compared with PYTHIA 8 Monash, PYTHIA 8 Shoving, PYTHIA 8 Ropes, PYTHIA 8 CLR-BLC 3, and EPOS4 for the HM I multiplicity class. The empty boxes are the systematic uncertainties of reported spectra ratios, and the bands represent the statistical uncertainties in the models.

the  $K/\pi$  ratios with increasing momentum ( $p_T > 0.5$  GeV/c). Compared to the other PYTHIA 8 tunes, the CLR-BLC 3 shows an improved qualitative description of the  $p/\pi$  ratios. EPOS4 predictions provide a better description of the data for both the  $K/\pi$  and  $p/\pi$  ratios compared to PYTHIA 8 tunes. It has also

been observed that none of the PYTHIA 8 tunes capture the low- $p_T$  depletion seen in high-multiplicity results compared to the V0M I class.

### 3.3 $p_T$ -integrated results

The  $p_T$ -integrated particle yields ( $dN/dy$ ) and mean transverse momentum ( $\langle p_T \rangle$ ) are evaluated by integrating the measured  $p_T$  spectra in the available  $p_T$  ranges, while the Lévy–Tsallis functional fits are used to extrapolate the contribution to the  $p_T$  region that is not covered by the measurements [60]. The corresponding values of  $dN/dy$  and  $\langle p_T \rangle$  for the different multiplicity classes are reported in Tab. 3.

**Table 3:**  $dN/dy$  and  $\langle p_T \rangle$  (GeV/c) measured in different high-multiplicity classes. The first error represents the statistical uncertainty and the second one is the systematic.

$\pi^+ + \pi^-$		
Multiplicity class	$dN/dy$	$\langle p_T \rangle$ (GeV/c)
HM I	$33.967 \pm 0.011 \pm 1.915$	$(6.234 \pm 0.004 \pm 0.160) \times 10^{-1}$
HM II	$30.709 \pm 0.006 \pm 1.750$	$(6.121 \pm 0.001 \pm 0.156) \times 10^{-1}$
HM III	$28.778 \pm 0.006 \pm 1.648$	$(6.049 \pm 0.001 \pm 0.153) \times 10^{-1}$
$K^+ + K^-$		
Multiplicity class	$dN/dy$	$\langle p_T \rangle$ (GeV/c)
HM I	$5.067 \pm 0.007 \pm 0.380$	$(10.862 \pm 0.012 \pm 0.274) \times 10^{-1}$
HM II	$4.492 \pm 0.004 \pm 0.343$	$(10.670 \pm 0.008 \pm 0.296) \times 10^{-1}$
HM III	$4.192 \pm 0.003 \pm 0.313$	$(10.500 \pm 0.007 \pm 0.276) \times 10^{-1}$
$p + \bar{p}$		
Multiplicity class	$dN/dy$	$\langle p_T \rangle$ (GeV/c)
HM I	$1.883 \pm 0.003 \pm 0.168$	$(13.637 \pm 0.024 \pm 0.416) \times 10^{-1}$
HM II	$1.696 \pm 0.002 \pm 0.151$	$(13.455 \pm 0.017 \pm 0.410) \times 10^{-1}$
HM III	$1.590 \pm 0.002 \pm 0.142$	$(13.163 \pm 0.017 \pm 0.396) \times 10^{-1}$

The fraction of the yields extrapolated with the functional fit are 9% for  $\pi$ , 6% for K, and 7% for p. The order of these fractions remains approximately the same across all multiplicity classes. To estimate the systematic uncertainties of the extrapolated fractions, alternative fit functions, including Bose–Einstein, Fermi–Dirac,  $p_T$  exponential, and Blast–Wave [46] are used. The extrapolated systematic uncertainties in the integrated yield range from 0.9% to 1.8% for the  $\pi$ , K, and p particles, while for the  $\langle p_T \rangle$ , they vary from 0.83% to 1.5%. The statistical and systematic uncertainties on the  $dN/dy$  and  $\langle p_T \rangle$  are calculated by using the same methods as described in Ref. [19, 20].

The  $p_T$ -integrated kaon-to-pion and proton-to-pion ratios measured in high-multiplicity pp collisions at  $\sqrt{s} = 13$  TeV are shown in Fig. 7. These results are also compared with those measured in pp, p–Pb, and Pb–Pb collisions at  $\sqrt{s_{NN}} = 7, 13, 5.02,$  and  $2.76$  TeV, respectively [8, 18–20, 39]. The measurements show good agreement, within systematic uncertainties, with previously published results. These measurements have extended the  $K/\pi$  and  $p/\pi$  ratios in pp collisions to higher multiplicities. A small increase in the  $K/\pi$  ratio by a factor of  $1.39 \pm 0.19$  is seen when moving from low-multiplicity pp to the highest multiplicities in Pb–Pb collisions, hints at strangeness enhancement [61]. Our results from high-multiplicity pp collisions follow this trend. The  $p/\pi$  ratio decreases by a factor of  $1.23 \pm 0.15$  from pp ( $\langle dN_{ch}/d\eta \rangle \sim 3.9$ ) to high-multiplicity Pb–Pb collisions, suggesting the antibaryon–baryon annihilation in heavy-ion collisions [62]. Our results for the  $p/\pi$  ratio follow the trend exhibited here. Furthermore, the measurements are compared with the predictions from PYTHIA 8 and EPOS4. The PYTHIA 8 Monash, Shoving, and Ropes tunes describe the integrated  $K/\pi$  ratio reasonably well (Fig. 7), although noticeable deviations are observed in the  $p_T$ -differential ratios (see Fig. 6). In contrast, the PYTHIA 8 CLR-BLC Mode 3 tune systematically underestimates the measured ratio, especially for

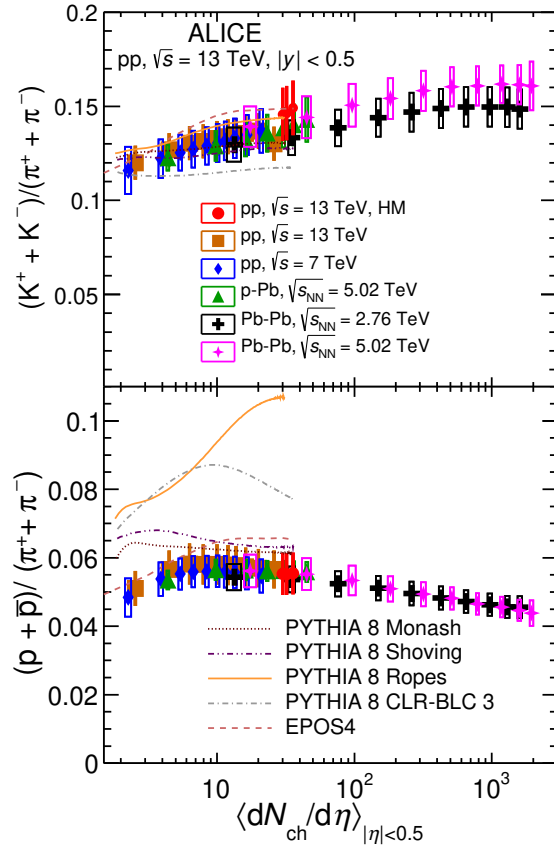


**Figure 7:**  $K/\pi$  (top) and  $p/\pi$  (bottom)  $p_T$ -integrated ratios as a function of  $\langle dN_{ch}/d\eta \rangle$  measured in pp, p–Pb, and Pb–Pb collisions at different center-of-mass energies [8, 18–20, 39]. Empty boxes represent the total systematic uncertainties and bars indicate the statistical ones. Colored lines represent the predictions from different tunes of PYTHIA 8 and EPOS4 for pp collisions at  $\sqrt{s} = 13$  TeV.

$\langle dN_{ch}/d\eta \rangle > 4$ . It should be noted that both PYTHIA 8 Monash and Shoving provide a qualitative description of the  $p/\pi$  ratio for  $\langle dN_{ch}/d\eta \rangle > 5$ . However, the PYTHIA 8 Ropes and PYTHIA 8 CLR-BLC 3 overestimate the data. EPOS4 describes the  $K/\pi$  ratio in the low ( $\langle dN_{ch}/d\eta \rangle < 6$ ) and high ( $\langle dN_{ch}/d\eta \rangle > 30$ ) multiplicity regions, while it reproduces the  $p/\pi$  ratio up to  $\langle dN_{ch}/d\eta \rangle \sim 8$ .

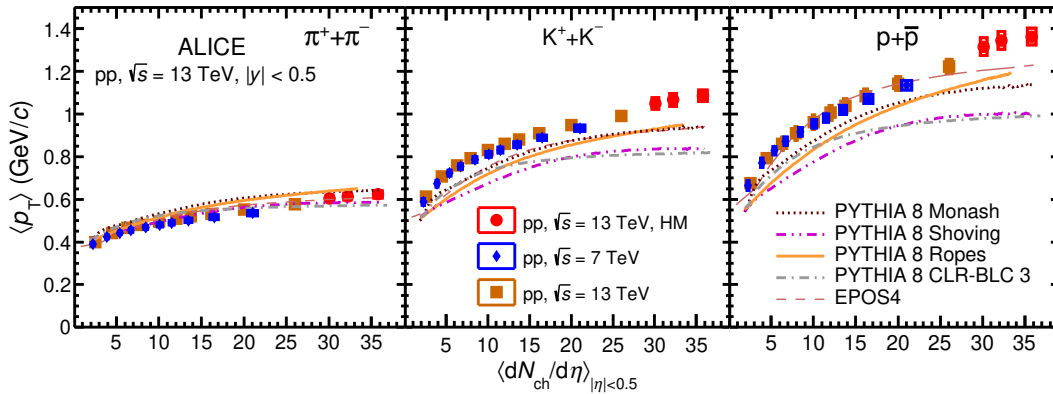


**Figure 8:**  $\langle p_T \rangle$  of  $\pi$ , K, and p as a function of  $\langle dN_{ch}/d\eta \rangle$  measured in pp collisions at  $\sqrt{s} = 7$  and 13 TeV [19, 20]. Open boxes indicate systematic uncertainties, and bars indicate the statistical ones. Colored lines represent the predictions from different tunes of PYTHIA 8 and EPOS4 for pp collisions at  $\sqrt{s} = 13$  TeV.

The  $\langle p_T \rangle$  of  $\pi$ , K and p as a function of  $\langle dN_{ch}/d\eta \rangle$  along with the published results of pp collisions at  $\sqrt{s} = 7$  and 13 TeV are shown in Fig. 8. A continuous increase in the  $\langle p_T \rangle$  with multiplicity is observed, and this increase is steeper for the hadrons with higher mass. The new results confirm this trend. This observation is the same as observed in heavy-ion collisions, which is consistent with radial flow effects. Comparing pp and Pb–Pb at similar multiplicity suggests that  $\langle p_T \rangle$  is higher in pp compared to that in Pb–Pb [19]. We also observe that all the models capture the increasing trend of  $\langle p_T \rangle$  with  $\langle dN_{ch}/d\eta \rangle$ . Among all the PYTHIA 8 tunes, PYTHIA 8 Shoving provides a quantitatively good description of the  $\langle p_T \rangle$  of pions, whereas all the tunes underestimate the kaon and proton  $\langle p_T \rangle$  values. The  $\langle p_T \rangle$  of pions predicted by EPOS4 is consistent with the data over the full range of  $\langle dN_{ch}/d\eta \rangle$ , whereas the  $\langle p_T \rangle$  of protons is well reproduced by EPOS4 up to  $\langle dN_{ch}/d\eta \rangle < 26$ , but is underestimated in the highest three multiplicity classes.

## 4 Conclusion

In this article, results related to the production of  $\pi$ , K, and p in high-multiplicity pp collisions at  $\sqrt{s} = 13$  TeV are presented. These new measurements have extended previous studies of pp collisions by pushing the average charged-particle multiplicity densities ( $\langle dN_{ch}/d\eta \rangle$ ) from 26.0 to 35.8, further bridging the gap between small and large collision systems. The transverse-momentum spectra, integrated yields, mean transverse momentum, and K/ $\pi$  and p/ $\pi$  ratios are presented. A comparison of these results with the published data for different system sizes and energies, and with the PYTHIA 8 (Monash, Shoving, Ropes and CLR-BLC 3 tunes) and EPOS4 models is presented.

A hardening of the  $p_T$  spectra across multiplicity classes is observed, which is more pronounced for particles with larger masses. The  $p_T$ -differential p/ $\pi$  ratio shows an enhancement at intermediate  $p_T$ , and the multiplicity-dependent K/ $\pi$  and p/ $\pi$  ratios display a smooth transition across different collision system sizes and energies. These results indicate that particle production is mainly driven by multiplicity, rather than by collision energy or system size. Furthermore, the  $\langle p_T \rangle$  as a function of  $\langle dN_{ch}/d\eta \rangle$  exhibits an increasing trend, with a more pronounced rise for heavier particles. These features, namely the hardening of  $p_T$  spectra with multiplicity and particle mass, the enhancement of the p/ $\pi$  ratio at intermediate  $p_T$ , and the increase of  $\langle p_T \rangle$ , are similar to those observed in heavy-ion collisions, where they are associated with the presence of radial flow. The PYTHIA 8 Monash and Ropes tunes qualitatively reproduce the pion spectra, while the Monash and Shoving tunes provide a reasonable description of the integrated K/ $\pi$  ratio. EPOS4 describes the increasing trend of the pion  $\langle p_T \rangle$  with multiplicity. Overall, EPOS4 captures the qualitative trends of the  $p_T$ -dependent K/ $\pi$  and p/ $\pi$  ratios more consistently than the PYTHIA 8 tunes.

## Acknowledgements

The ALICE Collaboration would like to thank all its engineers and technicians for their invaluable contributions to the construction of the experiment and the CERN accelerator teams for the outstanding performance of the LHC complex. The ALICE Collaboration gratefully acknowledges the resources and support provided by all Grid centres and the Worldwide LHC Computing Grid (WLCG) collaboration. The ALICE Collaboration acknowledges the following funding agencies for their support in building and running the ALICE detector: A. I. Alikhanyan National Science Laboratory (Yerevan Physics Institute) Foundation (ANSL), State Committee of Science and World Federation of Scientists (WFS), Armenia; Austrian Academy of Sciences, Austrian Science Fund (FWF): [M 2467-N36] and Nationalstiftung für Forschung, Technologie und Entwicklung, Austria; Ministry of Communications and High Technologies, National Nuclear Research Center, Azerbaijan; Rede Nacional de Física de Altas Energias (Renafae), Financiadora de Estudos e Projetos (Finep), Fundação de Amparo à Pesquisa do Estado de São Paulo (FAPESP) and The Sao Paulo Research Foundation (FAPESP), Brazil; Bulgarian Ministry

of Education and Science, within the National Roadmap for Research Infrastructures 2020-2027 (object CERN), Bulgaria; Ministry of Education of China (MOEC), Ministry of Science & Technology of China (MSTC) and National Natural Science Foundation of China (NSFC), China; Ministry of Science and Education and Croatian Science Foundation, Croatia; Centro de Aplicaciones Tecnológicas y Desarrollo Nuclear (CEADEN), Cubaenergía, Cuba; Ministry of Education, Youth and Sports of the Czech Republic, Czech Republic; The Danish Council for Independent Research | Natural Sciences, the VILLUM FONDEN and Danish National Research Foundation (DNRF), Denmark; Helsinki Institute of Physics (HIP), Finland; Commissariat à l’Energie Atomique (CEA) and Institut National de Physique Nucléaire et de Physique des Particules (IN2P3) and Centre National de la Recherche Scientifique (CNRS), France; Bundesministerium für Forschung, Technologie und Raumfahrt (BMFTR) and GSI Helmholtzzentrum für Schwerionenforschung GmbH, Germany; National Research, Development and Innovation Office, Hungary; Department of Atomic Energy Government of India (DAE), Department of Science and Technology, Government of India (DST), University Grants Commission, Government of India (UGC) and Council of Scientific and Industrial Research (CSIR), India; National Research and Innovation Agency - BRIN, Indonesia; Istituto Nazionale di Fisica Nucleare (INFN), Italy; Japanese Ministry of Education, Culture, Sports, Science and Technology (MEXT) and Japan Society for the Promotion of Science (JSPS) KAKENHI, Japan; Consejo Nacional de Ciencia (CONACYT) y Tecnología, through Fondo de Cooperación Internacional en Ciencia y Tecnología (FONCICYT) and Dirección General de Asuntos del Personal Académico (DGAPA), Mexico; Nederlandse Organisatie voor Wetenschappelijk Onderzoek (NWO), Netherlands; The Research Council of Norway, Norway; Pontificia Universidad Católica del Perú, Peru; Ministry of Science and Higher Education, National Science Centre and WUT ID-UB, Poland; Korea Institute of Science and Technology Information and National Research Foundation of Korea (NRF), Republic of Korea; Ministry of Education and Scientific Research, Institute of Atomic Physics, Ministry of Research and Innovation and Institute of Atomic Physics and Universitatea Nationala de Stiinta si Tehnologie Politehnica Bucuresti, Romania; Ministerstvo školstva, vyzkumu, vyvoja a mladeze SR, Slovakia; National Research Foundation of South Africa, South Africa; Swedish Research Council (VR) and Knut & Alice Wallenberg Foundation (KAW), Sweden; European Organization for Nuclear Research, Switzerland; Suranaree University of Technology (SUT), National Science and Technology Development Agency (NSTDA) and National Science, Research and Innovation Fund (NSRF via PMU-B B05F650021), Thailand; Turkish Energy, Nuclear and Mineral Research Agency (TENMAK), Turkey; National Academy of Sciences of Ukraine, Ukraine; Science and Technology Facilities Council (STFC), United Kingdom; National Science Foundation of the United States of America (NSF) and United States Department of Energy, Office of Nuclear Physics (DOE NP), United States of America. In addition, individual groups or members have received support from: FORTE project, reg. no. CZ.02.01.01/00/22\_008/0004632, Czech Republic, co-funded by the European Union, Czech Republic; European Research Council (grant no. 950692), European Union; Deutsche Forschungs Gemeinschaft (DFG, German Research Foundation) “Neutrinos and Dark Matter in Astro- and Particle Physics” (grant no. SFB 1258), Germany; FAIR - Future Artificial Intelligence Research, funded by the NextGenerationEU program (Italy).

## References

- [1] W. Busza, K. Rajagopal, and W. van der Schee, “Heavy Ion Collisions: The Big Picture and the Big Questions”, *Annu. Rev. Nucl. Part. Sci.* **68** (2018) 339–376, arXiv:1802.04801v2 [hep-ph].
- [2] U. Heinz and R. Snellings, “Collective Flow and Viscosity in Relativistic Heavy-Ion Collisions”, *Annu. Rev. Nucl. Part. Sci.* **63** (2013) 123–151, arXiv:1301.2826v1 [nucl-th].
- [3] J. E. Bernhard, J. S. Moreland, S. A. Bass, J. Liu, and U. Heinz, “Applying Bayesian parameter estimation to relativistic heavy-ion collisions: Simultaneous characterization of the initial state

- and quark–gluon plasma medium”, *Phys. Rev. C* **94** (2016) 024907, arXiv:1605.03954v2 [nucl-th].
- [4] F. G. Gardim, G. Giacalone, M. Luzum, and J.-Y. Ollitrault, “Thermodynamics of hot strong-interaction matter from ultrarelativistic nuclear collisions”, *Nat. Phys.* **16** (2020) 615–619, arXiv:1908.09728v2 [nucl-th].
- [5] P. Koch, B. Müller, and J. Rafelski, “Strangeness in relativistic heavy ion collisions”, *Phys. Rept.* **142** (1986) 167–262.
- [6] ALICE Collaboration, J. Adam *et al.*, “Anisotropic Flow of Charged Particles in Pb–Pb Collisions at  $\sqrt{s_{NN}} = 5.02$  TeV”, *Phys. Rev. Lett.* **116** (2016) 132302, arXiv:1602.01119 [nucl-ex].
- [7] ALICE Collaboration, J. Adam *et al.*, “Centrality dependence of the nuclear modification factor of charged pions, kaons, and protons in Pb–Pb collisions at  $\sqrt{s_{NN}} = 2.76$  TeV”, *Phys. Rev. C* **93** (2016) 034913, arXiv:1506.07287 [nucl-ex].
- [8] ALICE Collaboration, S. Acharya *et al.*, “Production of charged pions, kaons, and (anti-)protons in Pb–Pb and inelastic pp collisions at  $\sqrt{s_{NN}} = 5.02$  TeV”, *Phys. Rev. C* **101** (2020) 044907, arXiv:1910.07678 [nucl-ex].
- [9] CMS Collaboration, V. Khachatryan *et al.*, “Evidence for collectivity in pp collisions at the LHC”, *Phys. Lett. B* **765** (2017) 193–220, arXiv:1606.06198 [nucl-ex].
- [10] ALICE Collaboration, S. Acharya *et al.*, “Long- and short-range correlations and their event-scale dependence in high-multiplicity pp collisions at  $\sqrt{s} = 13$  TeV”, *JHEP* **05** (2021) 290, arXiv:2101.03110 [nucl-ex].
- [11] ALICE Collaboration, S. Acharya *et al.*, “Measurements of long-range two-particle correlation over a wide pseudorapidity range in p–Pb collisions at  $\sqrt{s_{NN}} = 5.02$  TeV”, *JHEP* **01** (2024) 199, arXiv:2308.16590 [nucl-ex].
- [12] ALICE Collaboration, S. Acharya *et al.*, “Multiplicity and event-scale dependent flow and jet fragmentation in pp collisions at  $\sqrt{s} = 13$  TeV and in p–Pb collisions at  $\sqrt{s_{NN}} = 5.02$  TeV”, *JHEP* **03** (2024) 092, arXiv:2308.16591 [nucl-ex].
- [13] ALICE Collaboration, J. Adam *et al.*, “Enhanced production of multi-strange hadrons in high-multiplicity proton–proton collisions”, *Nat. Phys.* **13** (2017) 535–539, arXiv:1606.07424 [nucl-ex].
- [14] ALICE Collaboration, J. Adam *et al.*, “Multi-strange baryon production in p–Pb collisions at  $\sqrt{s_{NN}} = 5.02$  TeV”, *Phys. Lett. B* **758** (2016) 389–401, arXiv:1512.07227 [nucl-ex].
- [15] CMS Collaboration, S. Chatrchyan *et al.*, “Observation of long-range near-side angular correlations in proton-lead collisions at the LHC”, *Phys. Lett. B* **718** (2013) 795–814, arXiv:1210.5482 [nucl-ex].
- [16] ALICE Collaboration, B. Abelev *et al.*, “Long-range angular correlations on the near and away side in p–Pb collisions at  $\sqrt{s_{NN}} = 5.02$  TeV”, *Phys. Lett. B* **719** (2013) 29–41, arXiv:1212.2001 [nucl-ex].
- [17] ALICE Collaboration, B. Abelev *et al.*, “Multi-particle azimuthal correlations in p–Pb and Pb–Pb collisions at the CERN Large Hadron Collider”, *Phys. Rev. C* **90** (2014) 054901, arXiv:1406.2474 [nucl-ex].

- [18] ALICE Collaboration, B. Abelev *et al.*, “Multiplicity dependence of pion, kaon, proton and lambda production in p–Pb collisions at  $\sqrt{s_{NN}} = 5.02$  TeV”, *Phys. Lett. B* **728** (2014) 25–38, arXiv:1307.6796 [nucl-ex].
- [19] ALICE Collaboration, S. Acharya *et al.*, “Multiplicity dependence of light-flavor hadron production in pp collisions at  $\sqrt{s} = 7$  TeV”, *Phys. Rev. C* **99** (2019) 024906, arXiv:1807.11321 [nucl-ex].
- [20] ALICE Collaboration, S. Acharya *et al.*, “Multiplicity dependence of  $\pi$ , K, and p production in pp collisions at  $\sqrt{s} = 13$  TeV”, *Eur. Phys. J. C* **80** (2020) 693, arXiv:2003.02394 [nucl-ex].
- [21] ALICE Collaboration, J. Adam *et al.*, “Multiplicity dependence of charged pion, kaon, and (anti)proton production at large transverse momentum in p–Pb collisions at  $\sqrt{s_{NN}} = 5.02$  TeV”, *Phys. Lett. B* **760** (2016) 720–735, arXiv:1601.03658 [nucl-ex].
- [22] ALICE Collaboration, B. Abelev *et al.*, “Production of charged pions, kaons and protons at large transverse momenta in pp and Pb–Pb collisions at  $\sqrt{s_{NN}} = 2.76$  TeV”, *Phys. Lett. B* **736** (2014) 196–207, arXiv:1401.1250 [nucl-ex].
- [23] T. Sjöstrand, S. Mrenna, and P. Skands, “PYTHIA 6.4 physics and manual”, *JHEP* **05** (2006) 026, arXiv:hep-ph/0603175 [hep-ph].
- [24] T. Sjöstrand, S. Mrenna, and P. Skands, “A brief introduction to PYTHIA 8.1”, *Comput. Phys. Commun.* **178** (2008) 852–867, arXiv:0710.3820 [hep-ph].
- [25] R. Corke and T. Sjöstrand, “Multiparton interactions with an x-dependent proton size”, *JHEP* **05** (2011) 009, arXiv:1101.5953 [hep-ph].
- [26] T. Pierog, I. Karpenko, J. M. Katzy, E. Yatsenko, and K. Werner, “EPOS LHC: Test of collective hadronization with data measured at the CERN Large Hadron Collider”, *Phys. Rev. C* **92** (2015) 034906, arXiv:1306.0121 [hep-ph].
- [27] K. Werner, I. Karpenko, T. Pierog, M. Bleicher, and K. Mikhailov, “Event-by-event simulation of the three-dimensional hydrodynamic evolution from flux tube initial conditions in ultrarelativistic heavy ion collisions”, *Phys. Rev. C* **82** (2010) 044904, arXiv:1004.0805 [nucl-th].
- [28] P. Skands, S. Carrazza, and J. Rojo, “Tuning PYTHIA 8.1: the Monash 2013 tune”, *Eur. Phys. J. C* **74** (2014) 3024, arXiv:1404.5630 [hep-ph].
- [29] A. Ortiz, G. Bencedi, and H. Bello, “Revealing the source of the radial flow patterns in proton–proton collisions using hard probes”, *J. Phys. G* **44** (2017) 065001, arXiv:1608.04784 [hep-ph].
- [30] N. Fischer and T. Sjöstrand, “Thermodynamical String Fragmentation”, *JHEP* **01** (2017) 140, arXiv:1610.09818 [hep-ph].
- [31] C. Bierlich, G. Gustafson, and L. Lönnblad, “Collectivity without plasma in hadronic collisions”, *Phys. Lett. B* **779** (2018) 58–63, arXiv:1710.09725 [hep-ph].
- [32] ALICE Collaboration, S. Acharya *et al.*, “Study of the flavor dependence of the baryon-to-meson ratio in proton–proton collisions at  $\sqrt{s} = 13$  TeV”, *Phys. Rev. D* **108** (2023) 112003, arXiv:2308.04873 [hep-ex].
- [33] K. Werner, “EPOS4: New theoretical concepts for modeling proton–proton and ion–ion scattering at very high energies”, arXiv:2410.09955 [hep-ph].

- [34] K. Werner, “Core-Corona Separation in Ultrarelativistic Heavy Ion Collisions”, *Phys. Rev. Lett.* **98** (2007) 152301, arXiv:0704.1270 [nucl-th].
- [35] K. Werner, “Core-corona procedure and microcanonical hadronization to understand strangeness enhancement in proton–proton and heavy ion collisions in the EPOS4 framework”, *Phys. Rev. C* **109** (2024) 014910, arXiv:2306.10277 [hep-ph].
- [36] ALICE Collaboration, S. Acharya *et al.*, “Light-flavor particle production in high-multiplicity pp collisions at  $\sqrt{s} = 13$  TeV as a function of transverse sphericity”, *JHEP* **05** (2024) 184, arXiv:2310.10236 [hep-ex].
- [37] ALICE Collaboration, K. Aamodt *et al.*, “The ALICE experiment at the CERN LHC”, *JINST* **3** (2008) S08002.
- [38] ALICE Collaboration, S. Acharya *et al.*, “The ALICE experiment: a journey through QCD”, *Eur. Phys. J. C* **84** (2024) 813, arXiv:2211.04384 [nucl-ex].
- [39] ALICE Collaboration, B. Abelev *et al.*, “Centrality dependence of  $\pi$ , K, and p production in Pb–Pb collisions at  $\sqrt{s_{NN}} = 2.76$  TeV”, *Phys. Rev. C* **88** (2013) 044910, arXiv:1303.0737 [hep-ex].
- [40] ALICE Collaboration, B. Abelev *et al.*, “Performance of the ALICE experiment at the CERN LHC”, *Int. J. Mod. Phys. A* **29** (2014) 1430044, arXiv:1402.4476 [nucl-ex].
- [41] ALICE Collaboration, K. Aamodt *et al.*, “Alignment of the ALICE Inner Tracking System with cosmic-ray tracks”, *JINST* **5** (2010) P03003, arXiv:1001.0502 [physics.ins-det].
- [42] J. Alme, Y. Andres, *et al.*, “The ALICE TPC, a large 3-dimensional tracking device with fast readout for ultra-high multiplicity events”, *Nucl. Instrum. Meth. A* **622** (2010) 316–367, arXiv:1001.1950 [physics.ins-det].
- [43] F. Carnesecchi, “Performance of the ALICE Time-Of-Flight detector at the LHC”, *JINST* **14** (2019) C06023, arXiv:1806.03825 [physics.ins-det].
- [44] ALICE Collaboration, E. Abbas *et al.*, “Mid-rapidity anti-baryon to baryon ratios in pp collisions at  $\sqrt{s} = 0.9, 2.76$  and 7 TeV measured by ALICE”, *Eur. Phys. J. C* **73** (2013) 2496, arXiv:1305.1562 [nucl-ex].
- [45] ALICE Collaboration, S. Acharya *et al.*, “Pseudorapidity distributions of charged particles as a function of mid- and forward rapidity multiplicities in pp collisions at  $\sqrt{s} = 5.02, 7$  and 13 TeV”, *Eur. Phys. J. C* **81** (2021) 630, arXiv:2009.09434 [nucl-ex].
- [46] ALICE Collaboration, S. Acharya *et al.*, “Multiplicity dependence of (multi-)strange hadron production in proton–proton collisions at  $\sqrt{s} = 13$  TeV”, *Eur. Phys. J. C* **80** (2020) 167, arXiv:1908.01861 [nucl-ex].
- [47] ALICE Collaboration, S. Acharya *et al.*, “Production of light (anti)nuclei in pp collisions at  $\sqrt{s} = 13$  TeV”, *JHEP* **01** (2022) 106, arXiv:2109.13026 [nucl-ex].
- [48] ALICE Collaboration, B. Abelev *et al.*, “Pseudorapidity density of charged particles in p–Pb collisions at  $\sqrt{s_{NN}} = 5.02$  TeV”, *Phys. Rev. Lett.* **110** (2013) 032301, arXiv:1210.3615 [nucl-ex].
- [49] ALICE Collaboration, J. Adam *et al.*, “Measurement of pion, kaon and proton production in proton–proton collisions at  $\sqrt{s} = 7$  TeV”, *Eur. Phys. J. C* **75** (2015) 226, arXiv:1504.00024 [nucl-ex].

- [50] ALICE Collaboration, S. Acharya *et al.*, “Production of light-flavor hadrons in pp collisions at  $\sqrt{s} = 7$  and  $\sqrt{s} = 13$  TeV”, *Eur. Phys. J. C* **81** (2021) 256, arXiv:2005.11120 [nucl-ex].
- [51] S. Agostinelli, et al., “Geant4—a simulation toolkit”, *Nucl. Instrum. Meth. A* **506** (2003) 250–303.
- [52] ALICE Collaboration, S. Acharya *et al.*, “The ALICE definition of primary particles, ALICE-PUBLIC-2017-005”, <https://cds.cern.ch/record/2270008>.
- [53] A. Ferrari, P. R. Sala, A. Fasso, and J. Ranft, “FLUKA: a multi-particle transport code (Program version 2005)”,.
- [54] ALICE Collaboration, K. Aamodt *et al.*, “Production of pions, kaons and protons in pp collisions at  $\sqrt{s} = 900$  GeV with ALICE at the LHC”, *Eur. Phys. J. C* **71** (2011) 1655, arXiv:1101.4110 [hep-ex].
- [55] C. Bierlich, G. Gustafson, L. Lönnblad, and A. Tarasov, “Effects of Overlapping Strings in pp Collisions”, *JHEP* **2015** (2015) 148, arXiv:1412.6259 [hep-ph].
- [56] J. R. Christiansen and P. Z. Skands, “String formation beyond leading colour”, *JHEP* **08** (2015) 003, arXiv:1505.01681 [hep-ph].
- [57] B. Andersson, G. Gustafson, and B. Soderberg, “A General Model for Jet Fragmentation”, *Z. Phys. C* **20** (1983) 317.
- [58] T. Sjostrand, “Jet Fragmentation of Nearby Partons”, *Nucl. Phys. B* **248** (1984) 469–502.
- [59] J. Kim, E.-J. Kim, S. Ji, and S. Lim, “Exploring the string shoving model in PYTHIA8 for collective behaviors in pp collisions”, *J. Korean Phys. Soc.* **79** (2021) 447–454, arXiv:2108.09686 [nucl-th].
- [60] C. Tsallis, “Possible generalization of Boltzmann-Gibbs statistics”, *J. Stat. Phys.* **52** (1988) 479–487.
- [61] J. Letessier and J. Rafelski, “Strangeness chemical equilibration in a quark-gluon plasma”, *Phys. Rev. C* **75** (2007) 014905.
- [62] V. Vovchenko and V. Koch, “Centrality dependence of proton and light nuclei yields as a consequence of baryon annihilation in the hadronic phase”, *Phys. Lett. B* **835** (2022) 137577, arXiv:2210.15641 [nucl-th].

## A The ALICE Collaboration

D.A.H. Abdallah<sup>134</sup>, I.J. Abualrob<sup>112</sup>, S. Acharya<sup>49</sup>, G. Aglieri Rinella<sup>32</sup>, L. Aglietta<sup>24</sup>, N. Agrawal<sup>25</sup>, Z. Ahammed<sup>132</sup>, S. Ahmad<sup>15</sup>, I. Ahuja<sup>36</sup>, Z. Akbar<sup>79</sup>, V. Akishina<sup>38</sup>, M. Al-Turany<sup>94</sup>, B. Alessandro<sup>55</sup>, R. Alfaro Molina<sup>66</sup>, B. Ali<sup>15</sup>, A. Alici<sup>1,25</sup>, J. Alme<sup>20</sup>, G. Alocco<sup>24</sup>, T. Alt<sup>63</sup>, I. Altsybeev<sup>92</sup>, C. Andrei<sup>44</sup>, N. Andreou<sup>111</sup>, A. Andronic<sup>123</sup>, M. Angeletti<sup>32</sup>, V. Angelov<sup>91</sup>, F. Antinori<sup>53</sup>, P. Antonioli<sup>50</sup>, N. Apadula<sup>71</sup>, H. Appelshäuser<sup>63</sup>, S. Arcelli<sup>1,25</sup>, R. Arnaldi<sup>55</sup>, I.C. Arsene<sup>19</sup>, M. Arslandok<sup>135</sup>, A. Augustinus<sup>32</sup>, R. Averbeck<sup>94</sup>, M.D. Azmi<sup>15</sup>, H. Baba<sup>121</sup>, A.R.J. Babu<sup>134</sup>, A. Badalà<sup>52</sup>, J. Bae<sup>100</sup>, Y. Bae<sup>100</sup>, Y.W. Baek<sup>100</sup>, X. Bai<sup>116</sup>, R. Bailhache<sup>63</sup>, Y. Bailung<sup>125</sup>, R. Bala<sup>88</sup>, A. Baldisseri<sup>127</sup>, B. Balis<sup>2</sup>, S. Bangalia<sup>114</sup>, Z. Banoo<sup>88</sup>, V. Barbasova<sup>36</sup>, F. Barile<sup>31</sup>, L. Barioglio<sup>55</sup>, M. Barlou<sup>24</sup>, B. Barman<sup>40</sup>, G.G. Barnaföldi<sup>45</sup>, L.S. Barnby<sup>111</sup>, E. Barreau<sup>99</sup>, V. Barret<sup>124</sup>, L. Barreto<sup>106</sup>, K. Barth<sup>32</sup>, E. Bartsch<sup>63</sup>, N. Bastid<sup>124</sup>, G. Batigne<sup>99</sup>, D. Battistini<sup>34,92</sup>, B. Batyunya<sup>139</sup>, L. Baudino<sup>24</sup>, D. Bauri<sup>46</sup>, J.L. Bazo Alba<sup>98</sup>, I.G. Bearden<sup>80</sup>, P. Becht<sup>94</sup>, D. Behera<sup>77,47</sup>, S. Behera<sup>46</sup>, I. Belikov<sup>126</sup>, V.D. Bella<sup>126</sup>, F. Bellini<sup>25</sup>, R. Bellwied<sup>112</sup>, L.G.E. Beltran<sup>105</sup>, Y.A.V. Beltran<sup>43</sup>, G. Bencedi<sup>45</sup>, O. Benchikhi<sup>73</sup>, A. Bensaoula<sup>112</sup>, S. Beole<sup>24</sup>, A. Berdnikova<sup>91</sup>, L. Bergmann<sup>71</sup>, L. Bernardinis<sup>23</sup>, L. Betev<sup>32</sup>, P.P. Bhaduri<sup>132</sup>, T. Bhalla<sup>87</sup>, A. Bhasin<sup>88</sup>, B. Bhattacharjee<sup>40</sup>, L. Bianchi<sup>24</sup>, J. Bielčík<sup>34</sup>, J. Bielčíková<sup>83</sup>, A. Bilandzic<sup>92</sup>, A. Binoy<sup>114</sup>, G. Biro<sup>45</sup>, S. Biswas<sup>4</sup>, M.B. Blidaru<sup>94</sup>, N. Bluhme<sup>38</sup>, C. Blume<sup>63</sup>, F. Bock<sup>84</sup>, T. Bodova<sup>20</sup>, L. Boldizsár<sup>45</sup>, M. Bombara<sup>36</sup>, P.M. Bond<sup>32</sup>, G. Bonomi<sup>131,54</sup>, H. Borel<sup>127</sup>, A. Borissov<sup>139</sup>, A.G. Borquez Carcamo<sup>91</sup>, E. Botta<sup>24</sup>, N. Bouchhar<sup>17</sup>, Y.E.M. Bouziani<sup>63</sup>, D.C. Brandibur<sup>62</sup>, L. Bratrud<sup>63</sup>, P. Braun-Munzinger<sup>94</sup>, M. Bregant<sup>106</sup>, M. Broz<sup>34</sup>, G.E. Bruno<sup>93,31</sup>, V.D. Buchakchiev<sup>35</sup>, M.D. Buckland<sup>82</sup>, H. Buesching<sup>63</sup>, S. Bufalino<sup>29</sup>, P. Buhler<sup>73</sup>, N. Burmasov<sup>139</sup>, Z. Buthelezi<sup>67,120</sup>, A. Bylinkin<sup>20</sup>, C. Carr<sup>97</sup>, J.C. Cabanillas Noris<sup>105</sup>, M.F.T. Cabrera<sup>112</sup>, H. Caines<sup>135</sup>, A. Caliva<sup>28</sup>, E. Calvo Villar<sup>98</sup>, J.M.M. Camacho<sup>105</sup>, P. Camerini<sup>23</sup>, M.T. Camerlingo<sup>49</sup>, F.D.M. Canedo<sup>106</sup>, S. Cannito<sup>23</sup>, S.L. Cantway<sup>135</sup>, M. Carabas<sup>109</sup>, F. Carnesecchi<sup>32</sup>, L.A.D. Carvalho<sup>106</sup>, J. Castillo Castellanos<sup>127</sup>, M. Castoldi<sup>32</sup>, F. Catalano<sup>32</sup>, S. Cattaruzzi<sup>23</sup>, R. Cerri<sup>24</sup>, I. Chakaberia<sup>71</sup>, P. Chakraborty<sup>133</sup>, J.W.O. Chan<sup>112</sup>, S. Chandra<sup>132</sup>, S. Chapeland<sup>32</sup>, M. Chartier<sup>115</sup>, S. Chattopadhyay<sup>132</sup>, M. Chen<sup>39</sup>, T. Cheng<sup>6</sup>, M.I. Cherciu<sup>62</sup>, C. Cheshkov<sup>125</sup>, D. Chiappara<sup>27</sup>, V. Chibante Barroso<sup>32</sup>, D.D. Chinellato<sup>73</sup>, F. Chinu<sup>24</sup>, E.S. Chizzali<sup>11,92</sup>, J. Cho<sup>57</sup>, S. Cho<sup>57</sup>, P. Chochula<sup>32</sup>, Z.A. Chochulska<sup>III,133</sup>, P. Christakoglou<sup>81</sup>, C.H. Christensen<sup>80</sup>, P. Christiansen<sup>72</sup>, T. Chujo<sup>122</sup>, B. Chytla<sup>133</sup>, M. Ciaccio<sup>24</sup>, C. Cicalo<sup>51</sup>, G. Cimaror<sup>32,24</sup>, F. Cindolo<sup>50</sup>, F. Colamaria<sup>49</sup>, D. Colella<sup>31</sup>, A. Colelli<sup>31</sup>, M. Colocci<sup>25</sup>, M. Concas<sup>32</sup>, G. Conesa Balbastre<sup>70</sup>, Z. Conesa del Valle<sup>128</sup>, G. Contin<sup>23</sup>, J.G. Contreras<sup>34</sup>, M.L. Coquet<sup>99</sup>, P. Cortese<sup>130,55</sup>, M.R. Cosentino<sup>108</sup>, F. Costa<sup>32</sup>, S. Costanza<sup>21</sup>, P. Crochet<sup>124</sup>, M.M. Czarnynoga<sup>133</sup>, A. Dainese<sup>53</sup>, E. Dall'occo<sup>32</sup>, G. Dange<sup>38</sup>, M.C. Danisch<sup>16</sup>, A. Danu<sup>62</sup>, A. Daribayeva<sup>38</sup>, P. Das<sup>32</sup>, S. Das<sup>4</sup>, A.R. Dash<sup>123</sup>, S. Dash<sup>46</sup>, A. De Caro<sup>28</sup>, G. de Cataldo<sup>49</sup>, J. de Cuveland<sup>38</sup>, A. De Falco<sup>22</sup>, D. De Gruttola<sup>28</sup>, N. De Marco<sup>55</sup>, C. De Martin<sup>23</sup>, S. De Pasquale<sup>28</sup>, R. Deb<sup>131</sup>, R. Del Grande<sup>34</sup>, L. Dello Stritto<sup>32</sup>, G.G.A. de Souza<sup>IV,106</sup>, P. Dhankher<sup>18</sup>, D. Di Bari<sup>31</sup>, M. Di Costanzo<sup>29</sup>, A. Di Mauro<sup>32</sup>, B. Di Ruzza<sup>I,129,49</sup>, B. Diab<sup>32</sup>, Y. Ding<sup>6</sup>, J. Ditzel<sup>63</sup>, R. Divià<sup>32</sup>, U. Dmitrieva<sup>55</sup>, A. Dobrin<sup>62</sup>, B. Dönigus<sup>63</sup>, L. Döpper<sup>41</sup>, L. Drzensla<sup>2</sup>, J.M. Dubinski<sup>133</sup>, A. Dubla<sup>94</sup>, P. Dupieux<sup>124</sup>, N. Dzalaiova<sup>13</sup>, T.M. Eder<sup>123</sup>, R.J. Ehlers<sup>71</sup>, F. Eisenhut<sup>63</sup>, R. Ejima<sup>89</sup>, D. Elia<sup>49</sup>, B. Erazmus<sup>99</sup>, F. Ercolessi<sup>25</sup>, B. Espagnon<sup>128</sup>, G. Eulisse<sup>32</sup>, D. Evans<sup>97</sup>, L. Fabbietti<sup>92</sup>, G. Fabbri<sup>50</sup>, M. Faggin<sup>32</sup>, J. Faivre<sup>70</sup>, W. Fan<sup>112</sup>, T. Fang<sup>6</sup>, A. Fantoni<sup>48</sup>, A. Feliciello<sup>55</sup>, W. Feng<sup>6</sup>, A. Fernández Téllez<sup>43</sup>, B. Fernando<sup>134</sup>, L. Ferrandi<sup>106</sup>, A. Ferrero<sup>127</sup>, C. Ferrero<sup>V,55</sup>, A. Ferretti<sup>24</sup>, D. Finogeev<sup>139</sup>, F.M. Fionda<sup>51</sup>, A.N. Flores<sup>104</sup>, S. Foertsch<sup>67</sup>, I. Fokin<sup>91</sup>, U. Follo<sup>V,55</sup>, R. Forynski<sup>111</sup>, E. Fragiaco<sup>56</sup>, H. Friberg<sup>92</sup>, U. Fuchs<sup>32</sup>, D. Fuligno<sup>23</sup>, N. Funicello<sup>28</sup>, C. Furget<sup>70</sup>, A. Furs<sup>139</sup>, T. Fusayasu<sup>95</sup>, J.J. Gaardhøje<sup>80</sup>, M. Gagliardi<sup>24</sup>, A.M. Gago<sup>98</sup>, T. Gahlaut<sup>46</sup>, C.D. Galvan<sup>105</sup>, S. Gami<sup>77</sup>, C. Garabatos<sup>94</sup>, J.M. Garcia<sup>43</sup>, E. Garcia-Solis<sup>9</sup>, S. Garetti<sup>128</sup>, C. Gargiulo<sup>32</sup>, P. Gasik<sup>94</sup>, A. Gautam<sup>114</sup>, M.B. Gay Ducati<sup>65</sup>, M. Germain<sup>99</sup>, R.A. Gernhaeuser<sup>92</sup>, M. Giacalone<sup>32</sup>, G. Gioachin<sup>29</sup>, S.K. Giri<sup>132</sup>, P. Giubellino<sup>55</sup>, P. Giubilato<sup>27</sup>, P. Glässel<sup>91</sup>, E. Glimos<sup>119</sup>, L. Gonella<sup>23</sup>, V. Gonzalez<sup>134</sup>, M. Gorgon<sup>2</sup>, K. Goswami<sup>47</sup>, S. Gotovac<sup>33</sup>, V. Grabski<sup>66</sup>, L.K. Graczykowski<sup>133</sup>, E. Grecka<sup>83</sup>, A. Grelli<sup>58</sup>, C. Grigoras<sup>32</sup>, S. Grigoryan<sup>139,1</sup>, O.S. Groettvik<sup>32</sup>, M. Gronbeck<sup>41</sup>, F. Grosa<sup>32</sup>, S. Gross-Bölting<sup>94</sup>, J.F. Grosse-Oetringhaus<sup>32</sup>, R. Grosso<sup>94</sup>, D. Grund<sup>34</sup>, N.A. Grunwald<sup>91</sup>, R. Guernane<sup>70</sup>, M. Guilbaud<sup>99</sup>, K. Gulbrandsen<sup>80</sup>, J.K. Gumprecht<sup>73</sup>, T. Gündem<sup>63</sup>, T. Gunji<sup>121</sup>, J. Guo<sup>10</sup>, W. Guo<sup>6</sup>, A. Gupta<sup>88</sup>, R. Gupta<sup>88</sup>, R. Gupta<sup>47</sup>, K. Gwizdziel<sup>133</sup>, L. Gyulai<sup>45</sup>, T. Hachiya<sup>75</sup>,

C. Hadjidakis<sup>128</sup>, F.U. Haider<sup>88</sup>, S. Haidlova<sup>34</sup>, M. Haldar<sup>4</sup>, W. Ham<sup>100</sup>, H. Hamagaki<sup>74</sup>, Y. Han<sup>137</sup>, R. Hannigan<sup>104</sup>, J. Hansen<sup>72</sup>, J.W. Harris<sup>135</sup>, A. Harton<sup>9</sup>, M.V. Hartung<sup>63</sup>, A. Hasan<sup>118</sup>, H. Hassan<sup>113</sup>, D. Hatzifotiadou<sup>50</sup>, P. Hauer<sup>41</sup>, L.B. Havener<sup>135</sup>, E. Hellbär<sup>32</sup>, H. Helstrup<sup>37</sup>, M. Hemmer<sup>63</sup>, S.G. Hernandez<sup>112</sup>, G. Herrera Corral<sup>8</sup>, K.F. Hetland<sup>37</sup>, B. Heybeck<sup>63</sup>, H. Hillemanns<sup>32</sup>, B. Hippolyte<sup>126</sup>, I.P.M. Hobus<sup>81</sup>, F.W. Hoffmann<sup>38</sup>, B. Hofman<sup>58</sup>, Y. Hong<sup>57</sup>, A. Horzyk<sup>2</sup>, Y. Hou<sup>94,11</sup>, P. Hristov<sup>32</sup>, L.M. Huhta<sup>113</sup>, T.J. Humanic<sup>85</sup>, V. Humlova<sup>34</sup>, M. Husar<sup>86</sup>, A. Hutson<sup>112</sup>, D. Hutter<sup>38</sup>, M.C. Hwang<sup>18</sup>, M. Inaba<sup>122</sup>, A. Isakov<sup>81</sup>, T. Isidori<sup>114</sup>, M.S. Islam<sup>46</sup>, M. Ivanov<sup>13</sup>, M. Ivanov<sup>94</sup>, K.E. Iversen<sup>72</sup>, J.G. Kim<sup>137</sup>, M. Jablonski<sup>2</sup>, B. Jacak<sup>18,71</sup>, N. Jacazio<sup>25</sup>, P.M. Jacobs<sup>71</sup>, A. Jadlovská<sup>102</sup>, S. Jadlovská<sup>102</sup>, S. Jaelani<sup>79</sup>, C. Jahnke<sup>107</sup>, M.J. Jakubowska<sup>133</sup>, E.P. Jamaro<sup>2</sup>, D.M. Janik<sup>34</sup>, M.A. Janik<sup>133</sup>, S. Ji<sup>16</sup>, Y. Ji<sup>94</sup>, S. Jia<sup>80</sup>, T. Jiang<sup>10</sup>, A.A.P. Jimenez<sup>64</sup>, S. Jin<sup>10</sup>, F. Jonas<sup>71</sup>, D.M. Jones<sup>115</sup>, J.M. Jowett<sup>32,94</sup>, J. Jung<sup>63</sup>, M. Jung<sup>63</sup>, A. Junique<sup>32</sup>, J. Juracka<sup>34</sup>, J. Kaewjai<sup>115,101</sup>, P. Kalinak<sup>59</sup>, A. Kalweit<sup>32</sup>, A. Karasu Uysal<sup>136</sup>, N. Karatzenis<sup>97</sup>, T. Karavicheva<sup>139</sup>, M.J. Karwowska<sup>133</sup>, V. Kashyap<sup>77</sup>, M. Keil<sup>32</sup>, B. Ketzer<sup>41</sup>, J. Keul<sup>63</sup>, S.S. Khade<sup>47</sup>, A.M. Khan<sup>116</sup>, A. Khuntia<sup>50</sup>, Z. Khuranova<sup>63</sup>, B. Kileng<sup>37</sup>, B. Kim<sup>100</sup>, D.J. Kim<sup>113</sup>, D. Kim<sup>100</sup>, E.J. Kim<sup>68</sup>, G. Kim<sup>57</sup>, H. Kim<sup>57</sup>, J. Kim<sup>137</sup>, J. Kim<sup>57</sup>, J. Kim<sup>32</sup>, M. Kim<sup>18</sup>, S. Kim<sup>17</sup>, T. Kim<sup>137</sup>, J.T. Kinner<sup>123</sup>, I. Kisel<sup>38</sup>, A. Kisiel<sup>133</sup>, J.L. Klay<sup>5</sup>, J. Klein<sup>32</sup>, S. Klein<sup>71</sup>, C. Klein-Bösing<sup>123</sup>, M. Kleiner<sup>63</sup>, A. Kluge<sup>32</sup>, M.B. Knuesel<sup>135</sup>, C. Kobdaj<sup>101</sup>, R. Kohara<sup>121</sup>, A. Kondratyev<sup>139</sup>, J. König<sup>63</sup>, P.J. Konopka<sup>32</sup>, G. Kornakov<sup>133</sup>, M. Korwieser<sup>92</sup>, C. Koster<sup>81</sup>, A. Kotliarov<sup>83</sup>, N. Kovacic<sup>86</sup>, M. Kowalski<sup>103</sup>, V. Kozuharov<sup>35</sup>, G. Kozlov<sup>38</sup>, I. Králik<sup>59</sup>, A. Kravčáková<sup>36</sup>, M.A. Krawczyk<sup>32</sup>, L. Krcal<sup>32</sup>, F. Krizek<sup>83</sup>, K. Krizkova Gajdosova<sup>34</sup>, C. Krug<sup>65</sup>, M. Krüger<sup>63</sup>, E. Kryshen<sup>139</sup>, V. Kučera<sup>57</sup>, C. Kuhn<sup>126</sup>, D. Kumar<sup>132</sup>, L. Kumar<sup>87</sup>, N. Kumar<sup>87</sup>, S. Kumar<sup>49</sup>, S. Kundu<sup>32</sup>, M. Kuo<sup>122</sup>, P. Kurashvili<sup>76</sup>, S. Kurita<sup>89</sup>, S. Kushpil<sup>83</sup>, A. Kuznetsov<sup>139</sup>, M.J. Kweon<sup>57</sup>, Y. Kwon<sup>137</sup>, S.L. La Pointe<sup>38</sup>, P. La Rocca<sup>26</sup>, A. Lakrathok<sup>101</sup>, S. Lambert<sup>99</sup>, A.R. Landou<sup>70</sup>, R. Langoy<sup>118</sup>, P. Larionov<sup>32</sup>, E. Laudi<sup>32</sup>, L. Lautner<sup>92</sup>, R.A.N. Laveaga<sup>105</sup>, R. Lavicka<sup>73</sup>, R. Lea<sup>131,54</sup>, J.B. Lebert<sup>38</sup>, H. Lee<sup>100</sup>, S. Lee<sup>57</sup>, I. Legrand<sup>44</sup>, G. Le gras<sup>123</sup>, A.M. Lejeune<sup>34</sup>, T.M. Lelek<sup>2</sup>, I. León Monzón<sup>105</sup>, M.M. Lesch<sup>92</sup>, P. Lévai<sup>45</sup>, M. Li<sup>6</sup>, P. Li<sup>10</sup>, X. Li<sup>10</sup>, B.E. Liang-Gilman<sup>18</sup>, J. Lien<sup>118</sup>, R. Lietava<sup>97</sup>, I. Likmeta<sup>112</sup>, B. Lim<sup>55</sup>, H. Lim<sup>16</sup>, S.H. Lim<sup>16</sup>, Y.N. Lima<sup>106</sup>, S. Lin<sup>10</sup>, V. Lindenstruth<sup>38</sup>, C. Lippmann<sup>94</sup>, D. Liskova<sup>102</sup>, D.H. Liu<sup>6</sup>, J. Liu<sup>115</sup>, Y. Liu<sup>6</sup>, G.S.S. Liveraro<sup>107</sup>, I.M. Lofnes<sup>20</sup>, C. Loizides<sup>20</sup>, S. Lokos<sup>103</sup>, J. Lömker<sup>58</sup>, X. Lopez<sup>124</sup>, E. López Torres<sup>7</sup>, C. Lotteau<sup>125</sup>, P. Lu<sup>116</sup>, W. Lu<sup>6</sup>, Z. Lu<sup>10</sup>, O. Luby nets<sup>94</sup>, G.A. Lucia<sup>29</sup>, F.V. Lugo<sup>66</sup>, J. Luo<sup>39</sup>, G. Luparello<sup>56</sup>, J. M. Friedrich<sup>92</sup>, Y.G. Ma<sup>39</sup>, V. Machacek<sup>80</sup>, M. Mager<sup>32</sup>, M. Mahlein<sup>92</sup>, A. Maire<sup>126</sup>, E. Majerz<sup>2</sup>, M.V. Makariev<sup>35</sup>, G. Malfattore<sup>50</sup>, N.M. Malik<sup>88</sup>, N. Malik<sup>15</sup>, D. Mallick<sup>128</sup>, N. Mallick<sup>113</sup>, G. Mandaglio<sup>30,52</sup>, S. Mandal<sup>77</sup>, S.K. Mandal<sup>76</sup>, A. Manea<sup>62</sup>, R. Manhart<sup>92</sup>, A.K. Manna<sup>47</sup>, F. Manso<sup>124</sup>, G. Mantzaridis<sup>92</sup>, V. Manzari<sup>49</sup>, Y. Mao<sup>6</sup>, R.W. Marcjan<sup>2</sup>, G.V. Margagliotti<sup>23</sup>, A. Margotti<sup>50</sup>, A. Marín<sup>94</sup>, C. Markert<sup>104</sup>, P. Martinengo<sup>32</sup>, M.I. Martínez<sup>43</sup>, M.P.P. Martins<sup>32,106</sup>, S. Masciocchi<sup>94</sup>, M. Masera<sup>24</sup>, A. Masoni<sup>51</sup>, L. Massacrier<sup>128</sup>, O. Massen<sup>58</sup>, A. Mastroserio<sup>129,49</sup>, L. Mattei<sup>24,124</sup>, S. Mattiazzo<sup>27</sup>, A. Matyja<sup>103</sup>, J.L. Mayo<sup>104</sup>, F. Mazzaschi<sup>32</sup>, M. Mazzilli<sup>31</sup>, Y. Melikyan<sup>42</sup>, M. Melo<sup>106</sup>, A. Menchaca-Rocha<sup>66</sup>, J.E.M. Mendez<sup>64</sup>, E. Meninno<sup>73</sup>, M.W. Menzel<sup>32,91</sup>, M. Meres<sup>13</sup>, L. Micheletti<sup>55</sup>, D. Mihai<sup>109</sup>, D.L. Mihaylov<sup>92</sup>, A.U. Mikalsen<sup>20</sup>, K. Mikhaylov<sup>139</sup>, L. Millot<sup>70</sup>, N. Minafra<sup>114</sup>, D. Miśkowiec<sup>94</sup>, A. Modak<sup>56</sup>, B. Mohanty<sup>77</sup>, M. Mohisin Khan<sup>VI,15</sup>, M.A. Molander<sup>42</sup>, M.M. Mondal<sup>77</sup>, S. Monira<sup>133</sup>, D.A. Moreira De Godoy<sup>123</sup>, A. Morsch<sup>32</sup>, C. Moscatelli<sup>23</sup>, T. Mrnjavac<sup>32</sup>, S. Mrozinski<sup>63</sup>, V. Muccifora<sup>48</sup>, S. Muhuri<sup>132</sup>, A. Mulliri<sup>22</sup>, M.G. Munhoz<sup>106</sup>, R.H. Munzer<sup>63</sup>, L. Musa<sup>32</sup>, J. Musinsky<sup>59</sup>, J.W. Myrcha<sup>133</sup>, B. Naik<sup>120</sup>, A.I. Nambrath<sup>18</sup>, B.K. Nandi<sup>46</sup>, R. Nania<sup>50</sup>, E. Nappi<sup>49</sup>, A.F. Nassirpour<sup>17</sup>, V. Nastase<sup>109</sup>, A. Nath<sup>91</sup>, N.F. Nathanson<sup>80</sup>, A. Neagu<sup>19</sup>, L. Nellen<sup>64</sup>, R. Nepeivoda<sup>72</sup>, S. Nese<sup>19</sup>, N. Nicassio<sup>31</sup>, B.S. Nielsen<sup>80</sup>, E.G. Nielsen<sup>80</sup>, F. Noferini<sup>50</sup>, S. Noh<sup>12</sup>, P. Nomokonov<sup>139</sup>, J. Norman<sup>115</sup>, N. Novitzky<sup>84</sup>, J. Nystrand<sup>20</sup>, M.R. Ockleton<sup>115</sup>, M. Ogino<sup>74</sup>, J. Oh<sup>16</sup>, S. Oh<sup>17</sup>, A. Ohlson<sup>72</sup>, M. Oida<sup>89</sup>, L.A.D. Oliveira<sup>107</sup>, C. Oppedisano<sup>55</sup>, A. Ortiz Velasquez<sup>64</sup>, H. Osanai<sup>74</sup>, J. Otwinowski<sup>103</sup>, M. Oya<sup>89</sup>, K. Oyama<sup>74</sup>, S. Padhan<sup>131,46</sup>, D. Pagano<sup>131,54</sup>, V. Pagliarino<sup>55</sup>, G. Paić<sup>64</sup>, A. Palasciano<sup>93,49</sup>, I. Panasenko<sup>72</sup>, P. Panigrahi<sup>46</sup>, C. Pantouvakis<sup>27</sup>, H. Park<sup>122</sup>, J. Park<sup>122</sup>, S. Park<sup>100</sup>, T.Y. Park<sup>137</sup>, J.E. Parkkila<sup>133</sup>, P.B. Pati<sup>80</sup>, Y. Patley<sup>46</sup>, R.N. Patra<sup>49</sup>, B. Paul<sup>132</sup>, F. Pazdic<sup>97</sup>, H. Pei<sup>6</sup>, T. Peitzmann<sup>58</sup>, X. Peng<sup>53,11</sup>, S. Perciballi<sup>24</sup>, G.M. Perez<sup>7</sup>, M. Petrovici<sup>44</sup>, S. Piano<sup>56</sup>, M. Pikna<sup>13</sup>, P. Pillot<sup>99</sup>, O. Pinazza<sup>50,32</sup>, C. Pinto<sup>32</sup>, S. Pisano<sup>48</sup>, M. Płoskoń<sup>71</sup>, A. Plachta<sup>133</sup>, M. Planinic<sup>86</sup>, D.K. Plociennik<sup>2</sup>, S. Politano<sup>32</sup>, N. Poljak<sup>86</sup>, A. Pop<sup>44</sup>, S. Porteboeuf-Houssais<sup>124</sup>, J.S. Potgieter<sup>110</sup>, I.Y. Pozos<sup>43</sup>,

K.K. Pradhan<sup>47</sup>, S.K. Prasad<sup>4</sup>, S. Prasad<sup>47</sup>, R. Preghenella<sup>50</sup>, F. Prino<sup>55</sup>, C.A. Pruneau<sup>134</sup>,  
 M. Puccio<sup>32</sup>, S. Pucillo<sup>28</sup>, S. Pulawski<sup>117</sup>, L. Quaglia<sup>24</sup>, A.M.K. Radhakrishnan<sup>47</sup>, S. Ragoni<sup>14</sup>,  
 A. Rai<sup>135</sup>, A. Rakotozafindrabe<sup>127</sup>, N. Ramasubramanian<sup>125</sup>, L. Ramello<sup>130,55</sup>, C.O. Ramírez-Álvarez<sup>43</sup>,  
 M. Rasa<sup>26</sup>, S.S. Räsänen<sup>42</sup>, R. Rath<sup>94</sup>, M.P. Rauch<sup>20</sup>, I. Ravasenga<sup>32</sup>, M. Razza<sup>25</sup>,  
 K.F. Read<sup>84,119</sup>, C. Reckziegel<sup>108</sup>, A.R. Redelbach<sup>38</sup>, K. Redlich<sup>VII,76</sup>, C.A. Reetz<sup>94</sup>,  
 H.D. Regules-Medel<sup>43</sup>, A. Rehman<sup>20</sup>, F. Reidt<sup>32</sup>, H.A. Reme-Ness<sup>37</sup>, K. Reygers<sup>91</sup>, M. Richter<sup>20</sup>,  
 A.A. Riedel<sup>92</sup>, W. Riegler<sup>32</sup>, A.G. Riffero<sup>24</sup>, M. Rignanese<sup>27</sup>, C. Ripoli<sup>28</sup>, C. Ristea<sup>62</sup>,  
 M.V. Rodríguez<sup>32</sup>, M. Rodríguez Cahuantzi<sup>43</sup>, K. Røed<sup>19</sup>, E. Rogochaya<sup>139</sup>, D. Rohr<sup>32</sup>,  
 D. Röhrich<sup>20</sup>, S. Rojas Torres<sup>34</sup>, P.S. Rokita<sup>133</sup>, G. Romanenko<sup>25</sup>, F. Ronchetti<sup>32</sup>, D. Rosales  
 Herrera<sup>43</sup>, E.D. Rosas<sup>64</sup>, K. Roslon<sup>133</sup>, A. Rossi<sup>53</sup>, A. Roy<sup>47</sup>, A. Roy<sup>118</sup>, S. Roy<sup>46</sup>, N. Rubini<sup>50</sup>,  
 O. Rubza<sup>15</sup>, J.A. Rudolph<sup>81</sup>, D. Ruggiano<sup>133</sup>, R. Rui<sup>23</sup>, P.G. Russek<sup>2</sup>, A. Rustamov<sup>78</sup>,  
 A. Rybicki<sup>103</sup>, L.C.V. Ryder<sup>114</sup>, G. Ryu<sup>69</sup>, J. Ryu<sup>16</sup>, W. Rzesza<sup>92</sup>, B. Sabiu<sup>50</sup>, R. Sadek<sup>71</sup>,  
 S. Sadhu<sup>41</sup>, A. Saha<sup>31</sup>, S. Saha<sup>77</sup>, B. Sahoo<sup>47</sup>, R. Sahoo<sup>47</sup>, D. Sahu<sup>64</sup>, P.K. Sahu<sup>60</sup>, J. Saini<sup>132</sup>,  
 S. Sakai<sup>122</sup>, S. Sambyal<sup>88</sup>, D. Samitz<sup>73</sup>, I. Sanna<sup>32</sup>, D. Sarkar<sup>80</sup>, V. Sarritzu<sup>22</sup>, V.M. Sarti<sup>92</sup>,  
 M.H.P. Sas<sup>81</sup>, U. Savino<sup>24</sup>, S. Sawan<sup>77</sup>, E. Scapparone<sup>50</sup>, J. Schambach<sup>84</sup>, H.S. Scheid<sup>32</sup>,  
 C. Schiaua<sup>44</sup>, R. Schicker<sup>91</sup>, F. Schlepper<sup>32,91</sup>, A. Schmah<sup>94</sup>, C. Schmidt<sup>94</sup>, M. Schmidt<sup>90</sup>,  
 J. Schoengarth<sup>63</sup>, R. Schotter<sup>73</sup>, A. Schröter<sup>38</sup>, J. Schukraft<sup>32</sup>, K. Schweda<sup>94</sup>, G. Scioli<sup>25</sup>,  
 E. Scomparin<sup>55</sup>, J.E. Seger<sup>14</sup>, D. Sekihata<sup>121</sup>, M. Selina<sup>81</sup>, I. Selyuzhenkov<sup>94</sup>, S. Senyukov<sup>126</sup>,  
 J.J. Seo<sup>91</sup>, L. Serkin<sup>VIII,64</sup>, L. Šerkšnytė<sup>32</sup>, A. Sevcenco<sup>62</sup>, T.J. Shaba<sup>67</sup>, A. Shabetai<sup>99</sup>,  
 R. Shahoyan<sup>32</sup>, B. Sharma<sup>88</sup>, D. Sharma<sup>46</sup>, H. Sharma<sup>53</sup>, M. Sharma<sup>88</sup>, S. Sharma<sup>88</sup>,  
 T. Sharma<sup>40</sup>, U. Sharma<sup>88</sup>, O. Sheibani<sup>134</sup>, K. Shigaki<sup>89</sup>, M. Shimomura<sup>75</sup>, Q. Shou<sup>39</sup>,  
 S. Siddhanta<sup>51</sup>, T. Siemiarczuk<sup>76</sup>, T.F. Silva<sup>106</sup>, W.D. Silva<sup>106</sup>, D. Silvermyr<sup>72</sup>,  
 T. Simantathammakul<sup>101</sup>, R. Simeonov<sup>35</sup>, B. Singh<sup>46</sup>, B. Singh<sup>88</sup>, B. Singh<sup>92</sup>, K. Singh<sup>47</sup>,  
 R. Singh<sup>77</sup>, R. Singh<sup>53</sup>, S. Singh<sup>15</sup>, T. Sinha<sup>96</sup>, B. Sitar<sup>13</sup>, M. Sitta<sup>130,55</sup>, T.B. Skaali<sup>19</sup>,  
 G. Skorodumovs<sup>91</sup>, N. Smirnov<sup>135</sup>, K.L. Smith<sup>16</sup>, R.J.M. Snellings<sup>58</sup>, E.H. Solheim<sup>19</sup>,  
 S. Solokhin<sup>81</sup>, C. Sonnabend<sup>32,94</sup>, J.M. Sonneveld<sup>81</sup>, F. Soramel<sup>27</sup>, A.B. Soto-Hernandez<sup>85</sup>,  
 R. Spijkers<sup>81</sup>, C. Sporleder<sup>113</sup>, I. Sputowska<sup>103</sup>, J. Staa<sup>72</sup>, J. Stachel<sup>91</sup>, L.L. Stahl<sup>106</sup>, I. Stan<sup>62</sup>,  
 A.G. Stejskal<sup>114</sup>, T. Stellhorn<sup>123</sup>, S.F. Stiefelmaier<sup>91</sup>, D. Stocco<sup>99</sup>, I. Storehaug<sup>19</sup>, N.J. Strangmann<sup>63</sup>,  
 P. Stratmann<sup>123</sup>, S. Strazzi<sup>25</sup>, A. Sturmiolo<sup>115,30,52</sup>, Y. Su<sup>6</sup>, A.A.P. Suaide<sup>106</sup>, C. Suire<sup>128</sup>,  
 A. Suiu<sup>109</sup>, M. Sukhanov<sup>139</sup>, M. Suljic<sup>32</sup>, V. Sumberia<sup>88</sup>, S. Sumowidagdo<sup>79</sup>, P. Sun<sup>10</sup>,  
 N.B. Sundstrom<sup>58</sup>, L.H. Tabares<sup>7</sup>, A. Tabikh<sup>70</sup>, S.F. Taghavi<sup>92</sup>, J. Takahashi<sup>107</sup>, M.A. Talamantes  
 Johnson<sup>43</sup>, G.J. Tambave<sup>77</sup>, Z. Tang<sup>116</sup>, J. Tanwar<sup>87</sup>, J.D. Tapia Takaki<sup>114</sup>, N. Tapus<sup>109</sup>,  
 L.A. Tarasovicova<sup>36</sup>, M.G. Tarzila<sup>44</sup>, A. Tauro<sup>32</sup>, A. Tavira García<sup>104,128</sup>, G. Tejeda Muñoz<sup>43</sup>,  
 L. Terlizzi<sup>24</sup>, C. Terrevoli<sup>49</sup>, D. Thakur<sup>55</sup>, S. Thakur<sup>4</sup>, M. Thogersen<sup>19</sup>, D. Thomas<sup>104</sup>,  
 A.M. Tiekoetter<sup>123</sup>, N. Tiltmann<sup>32,123</sup>, A.R. Timmins<sup>112</sup>, A. Toia<sup>63</sup>, R. Tokumoto<sup>89</sup>, S. Tomassini<sup>25</sup>,  
 K. Tomohiro<sup>89</sup>, Q. Tong<sup>6</sup>, V.V. Torres<sup>99</sup>, A. Trifiró<sup>30,52</sup>, T. Triloki<sup>93</sup>, A.S. Triolo<sup>32</sup>, S. Tripathy<sup>32</sup>,  
 T. Tripathy<sup>124</sup>, S. Trogolo<sup>24</sup>, V. Trubnikov<sup>3</sup>, W.H. Trzaska<sup>113</sup>, T.P. Trzcinski<sup>133</sup>, C. Tsolanta<sup>19</sup>,  
 R. Tu<sup>39</sup>, R. Turrisi<sup>53</sup>, T.S. Tveter<sup>19</sup>, K. Ullaland<sup>20</sup>, B. Ulukutlu<sup>92</sup>, S. Upadhyaya<sup>103</sup>, A. Uras<sup>125</sup>,  
 M. Urioni<sup>23</sup>, G.L. Usai<sup>22</sup>, M. Vaid<sup>88</sup>, M. Vala<sup>36</sup>, N. Valle<sup>54</sup>, L.V.R. van Doremalen<sup>58</sup>, M. van  
 Leeuwen<sup>81</sup>, C.A. van Veen<sup>91</sup>, R.J.G. van Weelden<sup>81</sup>, D. Varga<sup>45</sup>, Z. Varga<sup>135</sup>, P. Vargas Torres<sup>64</sup>,  
 O. Vázquez Doce<sup>48</sup>, O. Vazquez Rueda<sup>112</sup>, G. Vecil<sup>23</sup>, P. Veen<sup>127</sup>, E. Vercellin<sup>24</sup>, R. Verma<sup>46</sup>,  
 R. Vértesi<sup>45</sup>, M. Verweij<sup>58</sup>, L. Vickovic<sup>33</sup>, Z. Vilakazi<sup>120</sup>, A. Villani<sup>23</sup>, C.J.D. Villiers<sup>67</sup>, T. Virgili<sup>28</sup>,  
 M.M.O. Virta<sup>42</sup>, A. Vodopyanov<sup>139</sup>, M.A. Völkl<sup>97</sup>, S.A. Voloshin<sup>134</sup>, G. Volpe<sup>31</sup>, B. von Haller<sup>32</sup>,  
 I. Vorobyev<sup>32</sup>, N. Vozniuk<sup>139</sup>, J. Vrláková<sup>36</sup>, J. Wan<sup>39</sup>, C. Wang<sup>39</sup>, D. Wang<sup>39</sup>, Y. Wang<sup>116</sup>,  
 Y. Wang<sup>39</sup>, Y. Wang<sup>6</sup>, Z. Wang<sup>39</sup>, F. Weiglhofer<sup>32</sup>, S.C. Wenzel<sup>32</sup>, J.P. Wessels<sup>123</sup>, P.K. Wiacek<sup>2</sup>,  
 J. Wiechula<sup>63</sup>, J. Wikne<sup>19</sup>, G. Wilk<sup>76</sup>, J. Wilkinson<sup>94</sup>, G.A. Willems<sup>123</sup>, N. Wilson<sup>115</sup>,  
 B. Windelband<sup>91</sup>, J. Witte<sup>91</sup>, M. Wojnar<sup>2</sup>, C.I. Worek<sup>2</sup>, J.R. Wright<sup>104</sup>, C.-T. Wu<sup>6,27</sup>, W. Wu<sup>92,39</sup>,  
 Y. Wu<sup>116</sup>, K. Xiong<sup>39</sup>, Z. Xiong<sup>116</sup>, L. Xu<sup>125,6</sup>, R. Xu<sup>6</sup>, Z. Xue<sup>71</sup>, A. Yadav<sup>41</sup>, A.K. Yadav<sup>132</sup>,  
 Y. Yamaguchi<sup>89</sup>, S. Yang<sup>57</sup>, S. Yang<sup>20</sup>, S. Yano<sup>89</sup>, Z. Ye<sup>71</sup>, E.R. Yeats<sup>18</sup>, J. Yi<sup>6</sup>, R. Yin<sup>39</sup>,  
 Z. Yin<sup>6</sup>, I.-K. Yoo<sup>16</sup>, J.H. Yoon<sup>57</sup>, H. Yu<sup>12</sup>, S. Yuan<sup>20</sup>, A. Yuncu<sup>91</sup>, V. Zaccolo<sup>23</sup>, C. Zampolli<sup>32</sup>,  
 F. Zanone<sup>91</sup>, N. Zardoshti<sup>32</sup>, P. Závada<sup>61</sup>, B. Zhang<sup>91</sup>, C. Zhang<sup>127</sup>, L. Zhang<sup>39</sup>, M. Zhang<sup>124,6</sup>,  
 M. Zhang<sup>27,6</sup>, S. Zhang<sup>39</sup>, X. Zhang<sup>6</sup>, Y. Zhang<sup>116</sup>, Y. Zhang<sup>116</sup>, Z. Zhang<sup>6</sup>, D. Zhou<sup>6</sup>,  
 Y. Zhou<sup>80</sup>, Z. Zhou<sup>39</sup>, J. Zhu<sup>39</sup>, S. Zhu<sup>94,116</sup>, Y. Zhu<sup>6</sup>, A. Zingaretti<sup>27</sup>, S.C. Zugravel<sup>55</sup>, N. Zurlo<sup>131,54</sup>

## Affiliation Notes

<sup>I</sup> Deceased

<sup>II</sup> Also at: Max-Planck-Institut für Physik, Munich, Germany

<sup>III</sup> Also at: Czech Technical University in Prague (CZ)

<sup>IV</sup> Also at: Instituto de Física da Universidade de São Paulo

<sup>V</sup> Also at: Dipartimento DET del Politecnico di Torino, Turin, Italy

<sup>VI</sup> Also at: Department of Applied Physics, Aligarh Muslim University, Aligarh, India

<sup>VII</sup> Also at: Institute of Theoretical Physics, University of Wrocław, Poland

<sup>VIII</sup> Also at: Facultad de Ciencias, Universidad Nacional Autónoma de México, Mexico City, Mexico

## Collaboration Institutes

<sup>1</sup> A.I. Alikhanyan National Science Laboratory (Yerevan Physics Institute) Foundation, Yerevan, Armenia

<sup>2</sup> AGH University of Krakow, Cracow, Poland

<sup>3</sup> Bogolyubov Institute for Theoretical Physics, National Academy of Sciences of Ukraine, Kyiv, Ukraine

<sup>4</sup> Bose Institute, Department of Physics and Centre for Astroparticle Physics and Space Science (CAPSS), Kolkata, India

<sup>5</sup> California Polytechnic State University, San Luis Obispo, California, United States

<sup>6</sup> Central China Normal University, Wuhan, China

<sup>7</sup> Centro de Aplicaciones Tecnológicas y Desarrollo Nuclear (CEADEN), Havana, Cuba

<sup>8</sup> Centro de Investigación y de Estudios Avanzados (CINVESTAV), Mexico City and Mérida, Mexico

<sup>9</sup> Chicago State University, Chicago, Illinois, United States

<sup>10</sup> China Nuclear Data Center, China Institute of Atomic Energy, Beijing, China

<sup>11</sup> China University of Geosciences, Wuhan, China

<sup>12</sup> Chungbuk National University, Cheongju, Republic of Korea

<sup>13</sup> Comenius University Bratislava, Faculty of Mathematics, Physics and Informatics, Bratislava, Slovak Republic

<sup>14</sup> Creighton University, Omaha, Nebraska, United States

<sup>15</sup> Department of Physics, Aligarh Muslim University, Aligarh, India

<sup>16</sup> Department of Physics, Pusan National University, Pusan, Republic of Korea

<sup>17</sup> Department of Physics, Sejong University, Seoul, Republic of Korea

<sup>18</sup> Department of Physics, University of California, Berkeley, California, United States

<sup>19</sup> Department of Physics, University of Oslo, Oslo, Norway

<sup>20</sup> Department of Physics and Technology, University of Bergen, Bergen, Norway

<sup>21</sup> Dipartimento di Fisica, Università di Pavia, Pavia, Italy

<sup>22</sup> Dipartimento di Fisica dell'Università and Sezione INFN, Cagliari, Italy

<sup>23</sup> Dipartimento di Fisica dell'Università and Sezione INFN, Trieste, Italy

<sup>24</sup> Dipartimento di Fisica dell'Università and Sezione INFN, Turin, Italy

<sup>25</sup> Dipartimento di Fisica e Astronomia dell'Università and Sezione INFN, Bologna, Italy

<sup>26</sup> Dipartimento di Fisica e Astronomia dell'Università and Sezione INFN, Catania, Italy

<sup>27</sup> Dipartimento di Fisica e Astronomia dell'Università and Sezione INFN, Padova, Italy

<sup>28</sup> Dipartimento di Fisica 'E.R. Caianiello' dell'Università and Gruppo Collegato INFN, Salerno, Italy

<sup>29</sup> Dipartimento DISAT del Politecnico and Sezione INFN, Turin, Italy

<sup>30</sup> Dipartimento di Scienze MIFT, Università di Messina, Messina, Italy

<sup>31</sup> Dipartimento Interateneo di Fisica 'M. Merlin' and Sezione INFN, Bari, Italy

<sup>32</sup> European Organization for Nuclear Research (CERN), Geneva, Switzerland

<sup>33</sup> Faculty of Electrical Engineering, Mechanical Engineering and Naval Architecture, University of Split, Split, Croatia

<sup>34</sup> Faculty of Nuclear Sciences and Physical Engineering, Czech Technical University in Prague, Prague, Czech Republic

<sup>35</sup> Faculty of Physics, Sofia University, Sofia, Bulgaria

<sup>36</sup> Faculty of Science, P.J. Šafárik University, Košice, Slovak Republic

<sup>37</sup> Faculty of Technology, Environmental and Social Sciences, Bergen, Norway

<sup>38</sup> Frankfurt Institute for Advanced Studies, Johann Wolfgang Goethe-Universität Frankfurt, Frankfurt, Germany

<sup>39</sup> Fudan University, Shanghai, China

<sup>40</sup> Gauhati University, Department of Physics, Guwahati, India

<sup>41</sup> Helmholtz-Institut für Strahlen- und Kernphysik, Rheinische Friedrich-Wilhelms-Universität Bonn, Bonn,

## Germany

- 42 Helsinki Institute of Physics (HIP), Helsinki, Finland
- 43 High Energy Physics Group, Universidad Autónoma de Puebla, Puebla, Mexico
- 44 Horia Hulubei National Institute of Physics and Nuclear Engineering, Bucharest, Romania
- 45 HUN-REN Wigner Research Centre for Physics, Budapest, Hungary
- 46 Indian Institute of Technology Bombay (IIT), Mumbai, India
- 47 Indian Institute of Technology Indore, Indore, India
- 48 INFN, Laboratori Nazionali di Frascati, Frascati, Italy
- 49 INFN, Sezione di Bari, Bari, Italy
- 50 INFN, Sezione di Bologna, Bologna, Italy
- 51 INFN, Sezione di Cagliari, Cagliari, Italy
- 52 INFN, Sezione di Catania, Catania, Italy
- 53 INFN, Sezione di Padova, Padova, Italy
- 54 INFN, Sezione di Pavia, Pavia, Italy
- 55 INFN, Sezione di Torino, Turin, Italy
- 56 INFN, Sezione di Trieste, Trieste, Italy
- 57 Inha University, Incheon, Republic of Korea
- 58 Institute for Gravitational and Subatomic Physics (GRASP), Utrecht University/Nikhef, Utrecht, Netherlands
- 59 Institute of Experimental Physics, Slovak Academy of Sciences, Košice, Slovak Republic
- 60 Institute of Physics, Homi Bhabha National Institute, Bhubaneswar, India
- 61 Institute of Physics of the Czech Academy of Sciences, Prague, Czech Republic
- 62 Institute of Space Science (ISS), Bucharest, Romania
- 63 Institut für Kernphysik, Johann Wolfgang Goethe-Universität Frankfurt, Frankfurt, Germany
- 64 Instituto de Ciencias Nucleares, Universidad Nacional Autónoma de México, Mexico City, Mexico
- 65 Instituto de Física, Universidade Federal do Rio Grande do Sul (UFRGS), Porto Alegre, Brazil
- 66 Instituto de Física, Universidad Nacional Autónoma de México, Mexico City, Mexico
- 67 iThemba LABS, National Research Foundation, Somerset West, South Africa
- 68 Jeonbuk National University, Jeonju, Republic of Korea
- 69 Korea Institute of Science and Technology Information, Daejeon, Republic of Korea
- 70 Laboratoire de Physique Subatomique et de Cosmologie, Université Grenoble-Alpes, CNRS-IN2P3, Grenoble, France
- 71 Lawrence Berkeley National Laboratory, Berkeley, California, United States
- 72 Lund University Department of Physics, Division of Particle Physics, Lund, Sweden
- 73 Marietta Blau Institute, Vienna, Austria
- 74 Nagasaki Institute of Applied Science, Nagasaki, Japan
- 75 Nara Women's University (NWU), Nara, Japan
- 76 National Centre for Nuclear Research, Warsaw, Poland
- 77 National Institute of Science Education and Research, Homi Bhabha National Institute, Jatni, India
- 78 National Nuclear Research Center, Baku, Azerbaijan
- 79 National Research and Innovation Agency - BRIN, Jakarta, Indonesia
- 80 Niels Bohr Institute, University of Copenhagen, Copenhagen, Denmark
- 81 Nikhef, National institute for subatomic physics, Amsterdam, Netherlands
- 82 Nuclear Physics Group, STFC Daresbury Laboratory, Daresbury, United Kingdom
- 83 Nuclear Physics Institute of the Czech Academy of Sciences, Husinec-Řež, Czech Republic
- 84 Oak Ridge National Laboratory, Oak Ridge, Tennessee, United States
- 85 Ohio State University, Columbus, Ohio, United States
- 86 Physics department, Faculty of science, University of Zagreb, Zagreb, Croatia
- 87 Physics Department, Panjab University, Chandigarh, India
- 88 Physics Department, University of Jammu, Jammu, India
- 89 Physics Program and International Institute for Sustainability with Knotted Chiral Meta Matter (WPI-SKCM<sup>2</sup>), Hiroshima University, Hiroshima, Japan
- 90 Physikalisches Institut, Eberhard-Karls-Universität Tübingen, Tübingen, Germany
- 91 Physikalisches Institut, Ruprecht-Karls-Universität Heidelberg, Heidelberg, Germany
- 92 Physik Department, Technische Universität München, Munich, Germany
- 93 Politecnico di Bari and Sezione INFN, Bari, Italy
- 94 Research Division and ExtreMe Matter Institute EMMI, GSI Helmholtzzentrum für Schwerionenforschung

GmbH, Darmstadt, Germany

<sup>95</sup> Saga University, Saga, Japan

<sup>96</sup> Saha Institute of Nuclear Physics, Homi Bhabha National Institute, Kolkata, India

<sup>97</sup> School of Physics and Astronomy, University of Birmingham, Birmingham, United Kingdom

<sup>98</sup> Sección Física, Departamento de Ciencias, Pontificia Universidad Católica del Perú, Lima, Peru

<sup>99</sup> SUBATECH, IMT Atlantique, Nantes Université, CNRS-IN2P3, Nantes, France

<sup>100</sup> Sungkyunkwan University, Suwon City, Republic of Korea

<sup>101</sup> Suranaree University of Technology, Nakhon Ratchasima, Thailand

<sup>102</sup> Technical University of Košice, Košice, Slovak Republic

<sup>103</sup> The Henryk Niewodniczanski Institute of Nuclear Physics, Polish Academy of Sciences, Cracow, Poland

<sup>104</sup> The University of Texas at Austin, Austin, Texas, United States

<sup>105</sup> Universidad Autónoma de Sinaloa, Culiacán, Mexico

<sup>106</sup> Universidade de São Paulo (USP), São Paulo, Brazil

<sup>107</sup> Universidade Estadual de Campinas (UNICAMP), Campinas, Brazil

<sup>108</sup> Universidade Federal do ABC, Santo Andre, Brazil

<sup>109</sup> Universitatea Nationala de Stiinta si Tehnologie Politehnica Bucuresti, Bucharest, Romania

<sup>110</sup> University of Cape Town, Cape Town, South Africa

<sup>111</sup> University of Derby, Derby, United Kingdom

<sup>112</sup> University of Houston, Houston, Texas, United States

<sup>113</sup> University of Jyväskylä, Jyväskylä, Finland

<sup>114</sup> University of Kansas, Lawrence, Kansas, United States

<sup>115</sup> University of Liverpool, Liverpool, United Kingdom

<sup>116</sup> University of Science and Technology of China, Hefei, China

<sup>117</sup> University of Silesia in Katowice, Katowice, Poland

<sup>118</sup> University of South-Eastern Norway, Kongsberg, Norway

<sup>119</sup> University of Tennessee, Knoxville, Tennessee, United States

<sup>120</sup> University of the Witwatersrand, Johannesburg, South Africa

<sup>121</sup> University of Tokyo, Tokyo, Japan

<sup>122</sup> University of Tsukuba, Tsukuba, Japan

<sup>123</sup> Universität Münster, Institut für Kernphysik, Münster, Germany

<sup>124</sup> Université Clermont Auvergne, CNRS/IN2P3, LPC, Clermont-Ferrand, France

<sup>125</sup> Université de Lyon, CNRS/IN2P3, Institut de Physique des 2 Infinis de Lyon, Lyon, France

<sup>126</sup> Université de Strasbourg, CNRS, IPHC UMR 7178, F-67000 Strasbourg, France, Strasbourg, France

<sup>127</sup> Université Paris-Saclay, Centre d'Etudes de Saclay (CEA), IRFU, Département de Physique Nucléaire (DPhN), Saclay, France

<sup>128</sup> Université Paris-Saclay, CNRS/IN2P3, IJCLab, Orsay, France

<sup>129</sup> Università degli Studi di Foggia, Foggia, Italy

<sup>130</sup> Università del Piemonte Orientale, Vercelli, Italy

<sup>131</sup> Università di Brescia, Brescia, Italy

<sup>132</sup> Variable Energy Cyclotron Centre, Homi Bhabha National Institute, Kolkata, India

<sup>133</sup> Warsaw University of Technology, Warsaw, Poland

<sup>134</sup> Wayne State University, Detroit, Michigan, United States

<sup>135</sup> Yale University, New Haven, Connecticut, United States

<sup>136</sup> Yıldız Technical University, Istanbul, Turkey

<sup>137</sup> Yonsei University, Seoul, Republic of Korea

<sup>138</sup> Affiliated with an institute formerly covered by a cooperation agreement with CERN

<sup>139</sup> Affiliated with an international laboratory covered by a cooperation agreement with CERN.